Supporting Information

Single-Atom Effect on the Regulation of Buried Interface for Self-Assembled Molecules in Inverted Perovskite Solar Cells

Xingyu Liu,[a,+] Taiyu Wang,[a,+] Wenjie Chen,[a,+] Guosen Zhang,[a] Xiaofeng Li,[b] Xiaolei Lin,[b] Yue Wang,[a,*] Xiaozhen Huang,[a] Hongfang Du,[a] Mingwei An,[a,*] Diwei Zhang,[a,*] Yang Wang[a,c]*

[a] Strait Institute of Flexible Electronics (SIFE, Future Technologies), Fujian Key Laboratory of Flexible Electronics, Fujian Normal University and Strait Laboratory of Flexible Electronics (SLoFE), Fuzhou, Fujian 350117, China

[b] School of Aerospace Engineering, Xiamen University, Xiamen 361005, China

[c] State Key Laboratory of Structural Chemistry, Fujian Institute of Research on the Structure of Matter, Chinese Academy of Sciences, Fuzhou 350002, Fujian, China

[+] These authors contributed equally to this work.

* Corresponding author. E-mail: ifeywang@fjnu.edu.cn; ifedwzhang@fjnu.edu.cn; ifemwan@fjnu.edu.cn; ifewangy@fjnu.edu.cn

1. Experimental Section

1.1 Materials

All chemicals and reagents are purchased by Bidepharm and can be used without further purification unless otherwise stated. Solvents were purified using standard methods and dried if necessary. PbI_2 (99.99%), FAI (99.99%), CsI_2 (99.99%), MACl (99.99%), $PC_{61}BM$, and PEAI were purchased from Advanced Electron Technology Co., Ltd. Dimethyl sulfoxide (DMSO, 99.8%), N,N-dimethylformamide (DMF, 99.9%), Acetone, isopropyl alcohol (IPA, 99.9%), and chlorobenzene (CB, 99.8%) were purchased from Sigma-Aldrich. and used without further purification. Acetone (99%) and ethanol (99.7%) were purchased from Sinopharm Group. Indium tin oxide-coated glass (ITO glass) was produced by Advanced Electron Technology Co., Ltd.

Nickel oxide nanoparticle synthesis

5.81 g of $Ni(NO_3)_2 \cdot 6H_2O$ were dissolved in 20 mL of ultrapure water and stirred to obtain a green solution. Subsequently, 1.6 g of NaOH were dissolved in 4 mL of ultrapure water. The aqueous NaOH solution was then slowly added to the green $Ni(NO_3)_2 \cdot 6H_2O$ solution. The mixture was sealed and stirred for 20 min. The resulting colloidal precipitate was washed by centrifugation, dried in a vacuum freeze dryer for 24 h, and finally calcined in a tube furnace at 270 °C for 2 h to obtain the final product, NiO_x.

1.2 Synthesis
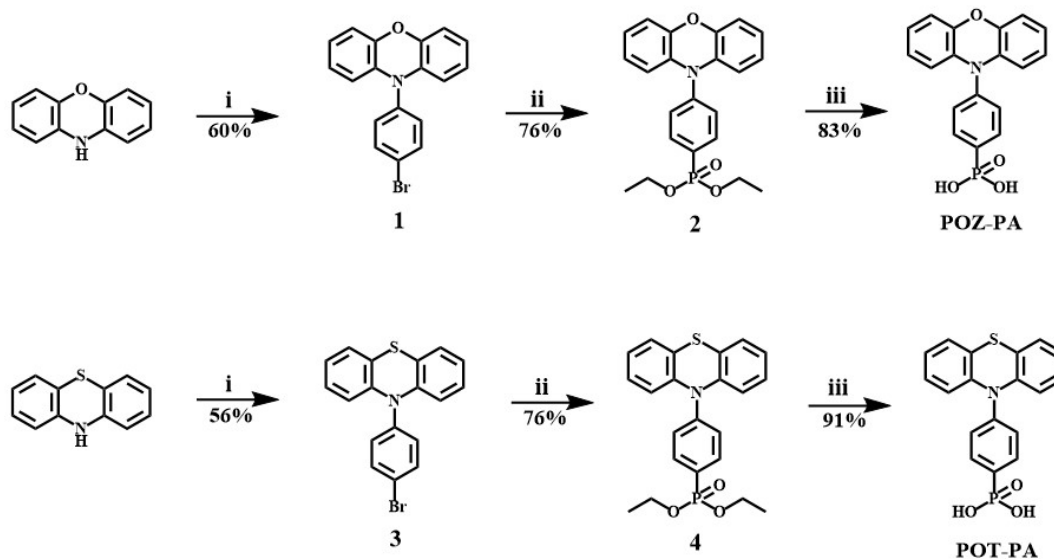
Scheme S1. The synthetic routes of POZ-PA and POT-PA SAMs. **i**: 4-Bromoiodobenzene, CuI (Copper(I) iodide), Sodium tert-butoxide, dioxane, 1,2-Diaminocyclohexane, 110 °C, 12 h; **ii:** Diethylphosphite, dppf (1,1′-Bis(diphenylphosphino)ferrocene), Pd(OAc)$_2$, KOAc, dioxane, 110 °C, 12 h; **iii:** Trimethylbromosilane, dioxane, room temperature, 12 h.

Compound 1[1]: Phenoxazine (10 mmol, 1.83 g), 4-Bromoiodobenzene (15 mmol, 4.23 g), Sodium tert-butoxide (20 mmol, 1.9 g), 1,2-Diaminocyclohexane (1 mmol, 120 μL), CuI (0.2 mmol, 38 mg), dioxane (20 mL) were added into a nitrogen filled bottom flask (100 mL), the mixture was heated to 110 °C overnight and then cooled to room temperature. The mixture was poured into water, extracted with DCM (dichloromethane), and the organic phase was dried over Na$_2$SO$_4$ (sodium sulfate). The product was purified by silica gel column chromatography using petroleum ether (PE) as the eluent with a yield of 60%. ^{1}H NMR (400 MHz, CDCl$_3$) δ 7.71 (d, J = 8.5 Hz, 2H), 7.22 (d, J = 8.5 Hz, 2H), 6.74-6.51 (m, 6H), 5.89 (m, 2H).

Compound 2[2]: Compound **1** (0.3 mmol, 200 mg) , diethyl phosphite (1.6 mmol, 0.3 mL), dppf (0.055 mmol, 30 mg), Pd(OAc)$_2$ (0.03 mmol, 5 mg), KOAc (2 mmol, 200 mg), dioxane (6 mL) were added into a nitrogen-filled bottom flask (25 mL), the mixture was heated to 110 °C overnight and then cooled to room temperature. The mixture was poured into water, extracted with DCM, and the organic phase was dried over Na$_2$SO$_4$. The product was purified by silica gel column chromatography using (DCM: EA (ethyl acetate) = 10:1) as the eluent with a yield of 76%. ^{1}H NMR (400 MHz, DMSO-d_6) δ 8.15-7.87 (m, 2H), 7.62 (d, J = 4.5 Hz, 2H), 6.78 (m, 3H), 6.70 (m, 3H), 5.89 (d, J = 7.4 Hz, 2H), 4.24-4.05 (m, 4H), 1.29 (t, J = 6.9 Hz, 6H). ^{13}C NMR (101 MHz, CDCl$_3$) δ 144.10, 134.71, 133.81, 131.23, 130.05, 128.16, 123.39, 121.95, 115.79, 113.42, 62.54, 16.52. ^{31}P NMR (162 MHz, DMSO-d_6) δ 16.73 (s, 1P). HRMS: C$_{18}$H$_{13}$O$_4$NP calcd: 396.13592, found: 396.13446 [M+H].

Compound POZ-PA[2]: Compound **2** (0.51 mmol, 200 mg), trimethylbromosilane (1 mL), and DCM (10 mL) were added into a nitrogen-filled bottom flask (25 mL) and stirred overnight at room temperature. After the reaction is complete, add methanol to quench any remaining reactive agents, evaporate the remaining solvent. The obtained solid was dissolved in a minimal amount of methanol, and the resulting solution was slowly poured into distilled water to induce precipitation. After thorough stirring and settling, the product was collected via filtration. The filter cake was sequentially washed with a DCM/ether mixed solvent system and subsequently dried under vacuum to yield the purple target compound with an isolated yield of 76%. ^{1}H NMR (400 MHz, DMSO-d_6) δ 7.94 (dd, J = 12.6, 7.9 Hz, 2H), 7.51 (d, J = 5.0 Hz, 2H), 6.76 (d, J = 5.0 Hz, 2H), 6.73-6.62 (m, 4H), 5.85 (d, J = 7.1 Hz, 2H). ^{13}C NMR (151 MHz, DMSO-d_6) δ 143.17, 140.72, 133.63, 133.55, 130.37, 130.28, 123.77, 121.73, 115.45, 113.26. ^{31}P NMR (162 MHz, DMSO-d_6) δ 11.42 (s, 1P). HRMS: C$_{18}$H$_{13}$O$_4$NP calcd: 338.05877, found: 338.05905 [M-H].

Compound 3[1]: It was prepared by similar methods as compound **1**. Yield: 56%. ^{1}H NMR (400 MHz, CDCl$_3$) δ 8.11 (d, J = 8.5 Hz, 2H), 7.67 (d, J = 6.6 Hz, 2H), 7.44 (d, J = 6.2 Hz, 2H), 7.32-7.20 (m, 4H), 6.64 (d, J = 7.9 Hz, 2H).

Compound 4[2]: It was prepared by similar methods as compound **2**. Yield: 76%. ^{1}H NMR (400 MHz, DMSO-d_6) δ 7.74 (dd, J = 12.6, 8.6 Hz, 2H), 7.39 (dd, J = 7.6, 1.3 Hz, 2H), 7.32-7.25 (m, 2H), 7.23 (dd, J = 7.7, 1.2 Hz, 2H), 7.14 (m, 2H), 6.93 (d,

J = 7.1 Hz, 2H), 4.01 (m, 4H), 1.24 (t, J = 7.0 Hz, 6H). ^{13}C NMR (101 MHz, CDCl$_3$) δ 142.41, 133.90, 133.79, 128.16, 127.24, 124.85, 124.39, 122.47, 122.30, 122.16, 62.26, 16.54. ^{31}P NMR (162 MHz, DMSO-d_6) δ 17.97 (s, 8P). HRMS: C$_{22}$H$_{23}$O$_3$NPS calcd: 412.11308, found: 412.11145 [M+H].

Compound POT-PA[2]: It was prepared by similar methods as compound **POZ-PA**. Yield: 91%. ^{1}H NMR (400 MHz, DMSO-d_6) δ 7.85 (dd, J = 12.6, 7.9 Hz, 2H), 7.40 (d, J = 5.1 Hz, 2H), 7.19 (d, J = 7.5 Hz, 2H), 7.05 (m, 2H), 6.96 (m, 2H), 6.43 (d, J = 8.2 Hz, 2H). ^{13}C NMR (101 MHz, DMSO-d_6) δ 142.84, 133.11, 133.01, 127.48, 127.22, 127.01, 126.87, 123.68, 122.45, 118.44. ^{31}P NMR (162 MHz, DMSO-d_6) δ 12.46 (s, 1P). HRMS: C$_{18}$H$_{13}$O$_3$NPS calcd: 354.03592, found: 354.03617 [M-H].
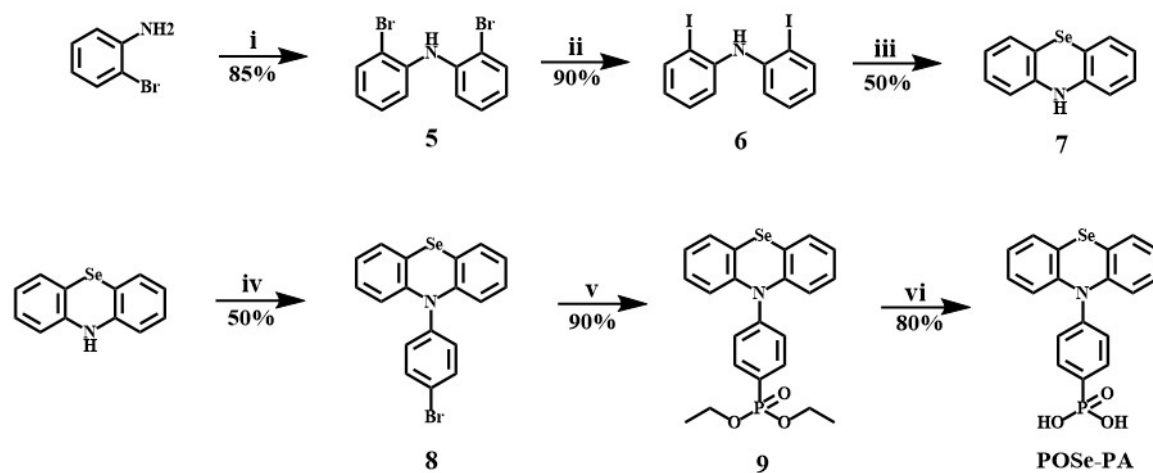
Scheme S2. The synthetic routes of POSe-PA SAMs. **i**: 2-Bromoaniline, 1-Bromo-2-iodobenzene, sodium tert-butoxide, dppf (1,1′-Bis(diphenylphosphino) ferrocene), Pd$_2$(dba)$_3$ (Tris(dibenzylideneacetone) dipalladium), toluene, 110 ℃, 12 h; **ii:** N,N′-Dimethyl-1, 2-ethanediamin, Sodium iodide, CuI, dioxane, 110 ℃, 24 h; **iii:** Selenium, KOH, DMSO, 120 ℃, 12 h; **iv**: 4-Bromoiodobenzene, CuI, sodium tert-butoxide, dioxane, 1,2-diaminocyclohexane, 110 ℃, 12 h; **v:** Diethylphosphite, dppf, Pd(OAc)$_2$, KOAc, dioxane, 110 ℃, 12 h; **vi**: Trimethylbromosilane, dioxane, room temperature, 12 h.

Compound 5[3]: 2-Bromoaniline (10 mmol, 1.72 g), 1-Bromo-2-iodobenzene (12 mmol, 3.39 g), dppf (1 mmol, 554 mg), Sodium tert-butoxide (15 mmol, 1.4 g),

Pd$_2$(dba)$_3$ (0.5 mmol, 458 mg), Toluene (20 mL) were added into a nitrogen filled bottom flask (100 mL), the mixture was heated to 120 °C overnight and then cooled to room temperature. The mixture was poured into water, extracted with DCM, and the organic phase was dried over Na$_2$SO$_4$. The product was purified by silica gel column chromatography using PE as the eluent with a yield of 85%. ^{1}H NMR (600 MHz, CDCl$_3$) δ 7.57 (m, 2H), 7.29 (m, 2H), 7.23-7.18 (m, 2H), 6.83 (m, 2H), 6.43 (s, 1H).

Compound 6[3]: Compound **5** (7 mmol, 2.25 g), Sodium iodide (28 mmol, 4.2 g), N,N'-Dimethyl-1,2-ethanediamin (1.84 mmol, 0.2 mL), CuI (0.92 mmol, 175 mg), dioxane (20 mL) were added into a nitrogen filled bottom flask (100 mL), the mixture was heated to 110 °C 24 h and then cooled to room temperature. The mixture was poured into water, extracted with DCM, and the organic phase was dried over Na$_2$SO$_4$. The product was purified by silica gel column chromatography using PE as the eluent with a yield of 92%. ^{1}H NMR (400 MHz, CDCl$_3$) δ 7.83 (dd, J = 8.0, 1.4 Hz, 2H), 7.25-7.22 (m, 2H), 7.17 (dd, J = 8.1, 1.6 Hz, 2H), 6.73-6.69 (m, 2H), 6.18 (s, 1H).

Compound 7[4]: Compound **6** (5.83 mmol, 2.5 g), selenium (12 mmol, 950 mg), KOH (24 mmol, 1.5 g), DMSO (20 mL) were added into a nitrogen filled bottom flask (100 mL), the mixture was heated to 120 °C overnight and then cooled to room temperature. The mixture was poured into water, extracted with DCM, and the organic phase was dried over Na$_2$SO$_4$. The product was purified by silica gel column chromatography using PE as the eluent with a yield of 45%. ^{1}H NMR (400 MHz, CDCl$_3$) δ 7.17 (dd, J = 7.6, 1.5 Hz, 2H), 7.07-7.03 (m, 2H), 6.87-6.83 (m, 2H), 6.64 (dd, J = 7.9, 1.3 Hz, 2H), 5.95 (s, 1H).

Compound 8[1]: It was prepared by similar methods as compound **1**. Yield: 52%. ^{1}H NMR (400 MHz, CDCl$_3$) δ 7.50 (d, J = 8.8 Hz, 2H), 7.39 (dd, J = 7.6, 1.6 Hz, 2H), 7.17-7.10 (m, 2H), 7.07 (d, J = 8.8 Hz, 2H), 7.03-6.99 (m, 2H), 6.87 (d, J = 8.1 Hz, 2H).

Compound 9[2]: It was prepared by similar methods as compound **2**. Yield: 78%. ^{1}H NMR (400 MHz, DMSO-d_6) δ 7.75 (d, J = 7.7 Hz, 2H), 7.57 (d, J = 7.9 Hz, 2H), 7.54-7.43 (m, 4H), 7.29 (m, 2H), 6.88 (dd, J = 8.7, 3.1 Hz, 2H), 4.00-3.85 (m, 4H), 1.18 (t, J = 7.0 Hz, 6H). ^{13}C NMR (101 MHz, CDCl$_3$) δ 141.39, 133.41, 131.66, 128.17, 127.93, 126.69, 126.45, 120.91, 114.38, 109.65, 61.99, 16.43. ^{31}P NMR (162 MHz, DMSO-d_6) δ 19.12 (s, 1P). HRMS: C$_{12}$H$_{23}$O$_3$NPSe calcd: 460.05753, found: 460.05596 [M+H].

Compound POSe-PA[2]: It was prepared by similar methods as compound **POZ-PA**. Yield: 60%. ^{1}H NMR (400 MHz, DMSO-d_6) δ 7.61 (d, J = 7.7 Hz, 2H), 7.52 (dd, J = 12.4, 8.2 Hz, 2H), 7.32 (m, 2H), 7.25 (d, J = 8.0 Hz, 2H), 7.17 (m, 2H), 6.94 (d, J = 8.6 Hz, 2H). ^{13}C NMR (101 MHz, DMSO-d_6) δ 141.61, 132.26, 132.15, 131.14, 128.04, 127.57, 125.98, 125.87, 117.40, 117.26. ^{31}P NMR (162 MHz, DMSO-d_6) δ 13.73(s, 1P). HRMS: $C_{18}H_{13}O_3NPSe$ calcd: 401.98037, found: 401.98004 [M-H].
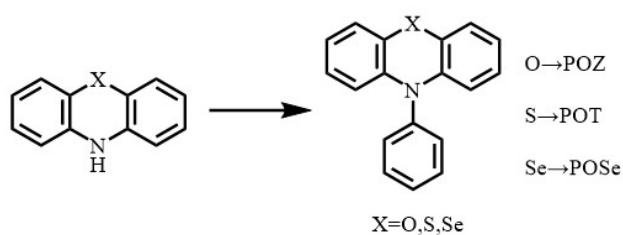
Scheme S3. The synthetic routes of POZ, POT and POSe. Reagents and conditions: iodobenzene, CuI, sodium tert-butoxide, 1,2-diaminocyclohexane, dioxane, 110 ℃, 12 h.

Compound POZ[1]: Phenoxazine (1 mmol, 183 mg), Iodobenzene (2 mmol, 400 mg), Sodium tert-butoxide (4 mmol, 400 mg), 1,2-Diaminocyclohexane (0.1 mmol, 12 μL), CuI (0.05 mmol, 10 mg), dioxane (5 mL) were added into a nitrogen filled bottom flask (100 mL), the mixture was heated to 110 ℃ overnight and then cooled to room temperature. The mixture was poured into water, extracted with DCM, and the organic phase was dried over Na_2SO_4. The product was purified by silica gel column chromatography using PE as the eluent with a yield of 55%. ^{1}H NMR (400 MHz, CDCl3) δ 7.66 (d, J = 7.7 Hz, 2H), 7.61-7.51 (m, 1H), 7.41 (d, J = 6.6 Hz, 2H), 6.77-6.70 (m, 2H), 6.70- 6.61 (m, 4H), 5.86-5.80 (m, 2H).

Compound POT[1]: It was prepared by similar methods as compound PO Z.Yield: 40%. ^{1}H NMR (400 MHz, DMSO-d_6) δ 7.69-7.65 (m, 2H), 7.56-7.52 (m, 1H), 7.42 (d, J = 7.1 Hz, 2H), 7.08 (dd, J = 7.5, 1.6 Hz, 2H), 6.97-6.91 (m, 2H), 6.88-6.86 (m, 2H), 6.16 (dd, J = 8.1, 1.3 Hz, 2H).

Compound POSe[1]: It was prepared by similar methods as compound PO Z.Yield: 60%. ^1H NMR (400 MHz, DMSO-d_6) δ 7.54-7.50 (m, 2H), 7.40 (d, J = 7.6 Hz, 2H), 7.38-7.32 (m, 1H), 7.26 (d, J = 8.6 Hz, 2H), 7.14-7.08 (m, 2 H), 7.02-6.96 (m, 2H), 6.68 (d, J = 8.2 Hz, 2H).

1.3 Theoretical Calculations

The ground-state geometry optimization was calculated using the density functional theory (DFT) method at the B3LYP/def2-SVP level of theory with the Gaussian 09 program package.[4] Stationary points were verified by frequency analysis. The optimized structures were found to be stable. The calculated molecular electronic static potential (ESP) results were obtained with the Multiwfn 3.7 program.[5]

1.4 Characterization and Measurements

The ^1H NMR, ^{13}C NMR, ^{31}P NMR and HRMS spectra were performed on the Bruker AVANCE III 500 MHz spectrometer. High-resolution mass spectra were obtained with ThermoScientificTM QExactive. Thermogravimetric (TGA) measurements were carried out on a METTLER TOLEDO (TGA 1 STARe System) apparatus at a heat ramp of 10 °C/min under N_2. Ultraviolet-visible (UV-Vis) absorption spectra were recorded on a Cary 5000 spectrophotometer. Steady-state photoluminescence (PL) (excitation wavelength 460 nm) and time-resolved photoluminescence (TRPL) were conducted with Edinburgh Instruments LTD (FLS 980). X-ray diffraction (XRD) was measured with a PANalytical X'Pert3 powder diffractometer equipped with a Cu-sealed tube (λ = 1.541874 Å) at 40 kV and 40 mA. The top-view and cross-section morphologies of the perovskite films were investigated using field emission scanning electron microscopy (SEM) (Apreo S LoVac, Thermo). The surface roughness and surface potential of perovskite films by atom force microscopy (AFM) and kelvin probe force microscopy (KPFM) were carried out using Oxford Jupiter XR. Fourier transform infrared (FTIR) spectra were characterized on a Thermo iS50 spectrometer with an ATR accessory. The testing samples of the mixtures of PbI_2 and each resonance molecule all have a molar ratio of 10:1. X-ray photoelectron spectroscopy (XPS) and ultraviolet photoelectron

spectroscopy (UPS) were obtained using ESCALAB Xi$^+$ XPS system (Thermo Fisher Scientific) with Al Kα X-ray radiation (1486.6 eV), UPS using a non-monochromated He photon source (hv = 21.22 eV). Current density-voltage (J-V) characteristics were measured using a Keithley 2401 SourceMeter under 100 mW×cm^{-2} simulated AM 1.5 G irradiation with a solar simulator (Enli Tech, Taiwan). The light source was warmed up for 20 min and equipped with a calibrated Si reference cell (SRC-2020, Enlitech) to correct the light intensity before the J-V test. The active area of devices was defined by a metal shadow mask of 0.1 cm^2. External quantum efficiency (EQE) was characterized by the quantum efficiency instrument (QE-R, Enlitech.), and the measurement scope was 300-850 nm. Electrochemical impedance (EIS) and Mott-Schottky measurements were tested in the dark using an electrochemical workstation (Zennium Zahner, Germany) at room temperature with 40% humidity. Space-charge limited current (SCLC) measurement was performed on a Keithley 2401 source meter ranging from 0 V to 3 V. Dark J-V curves of the hole-only devices (ITO/NiO$_x$/SAM/Perovskite/Spiro-OMeTAD/Ag) to evaluate the conductivity were measured by a Keithley 2401 source meter in the range of (-2) - (+2) V.

1.5 Device Fabrication

The ITO substrates were sequentially cleaned with detergent, deionized water, ethanol, acetone, and isopropanol by ultrasonication for 30 min in each solvent. The cleaned ITO substrates were then dried with N$_2$ and treated with UV ozone for 20 min before use. NiO$_x$ nanoparticles were dispersed in deionized water at a concentration of 10 mg/mL to form NiO$_x$ ink. The as-prepared NiO$_x$ ink was spin-coated onto the ITO substrate at 2000 rpm for 30 s, then annealing at 120 °C for 20 min in ambient air. Then NiO$_x$ substrates were transported into a N$_2$-filled glovebox. For the three SAMs with 0.5 mg/mL in ethanol were respectively spin-coated at the NiO$_x$ substrate at 3000 rpm for 30 s and annealed at 100 °C for 10 min. For deposition of perovskite layer, 1.5 M FA$_{0.95}$CS$_{0.05}$PbI$_3$ precursor solution with 5% excess PbI$_2$ and 10% MACl in 1 mL of a mixed anhydrous solvent of DMF and DMSO. The ratio of the solvents was fixed at 4/1 (DMF/DMSO) by volume. The perovskite precursor solution was spin-coated at 1000 rpm for 10 s and then at 4000 rpm for 40 s. During the second spin

coating step, 250 μL CB was dropped onto the perovskite film at 10 s before ending the program. The resultant wet perovskite films were annealed at 110 °C for 30 min. After that, 1.25 mg/mL PEAI was coated on the perovskite surface at 6000 rpm for 30 s and annealed at 80 °C for 5 min subsequently, the $PC_{61}BM$ solution in CB (2 mg/mL) was spin-coated on the perovskite films at 6000 rpm for 30 s and annealed at 80 °C for 10 min C_{60} (25 nm) and BCP (7 nm) layers were successively formed by thermally evaporating. Finally, approximately 100 nm Ag electrodes were deposited on top of the BCP layer by thermal evaporation under a high vacuum.

1.6 Stability Measurement

The long-term stability assessment of perovskite solar cells was conducted through repeated *J-V* characteristic curve measurements. For the thermal stability test, unencapsulated devices were stored in dark conditions at 60 °C (nitrogen atmosphere). For the storage stability test, unencapsulated devices were kept in dark ambient conditions at room temperature (nitrogen atmosphere).

1.7 Supplemental Notes

Supplementary Note 1: Calculation of the defect density (N_t)

Trap densities (N_t) of devices employed on hole-only devices with the structures of ITO/NiO$_x$/SAM/Perovskite/Spiro-OMeTAD/Ag. According to the formula[6]:

$$N_t = \frac{2\varepsilon_0\varepsilon_r V_{TFL}}{eL^2}$$

Where ε_0 is the vacuum permittivity, ε_r is the relative dielectric constant, V_{TFL} is the transition voltage between ohmic and trap-filling regions, e is the electron charge, and L is the perovskite film thickness.

2. Additional Figures and Tables
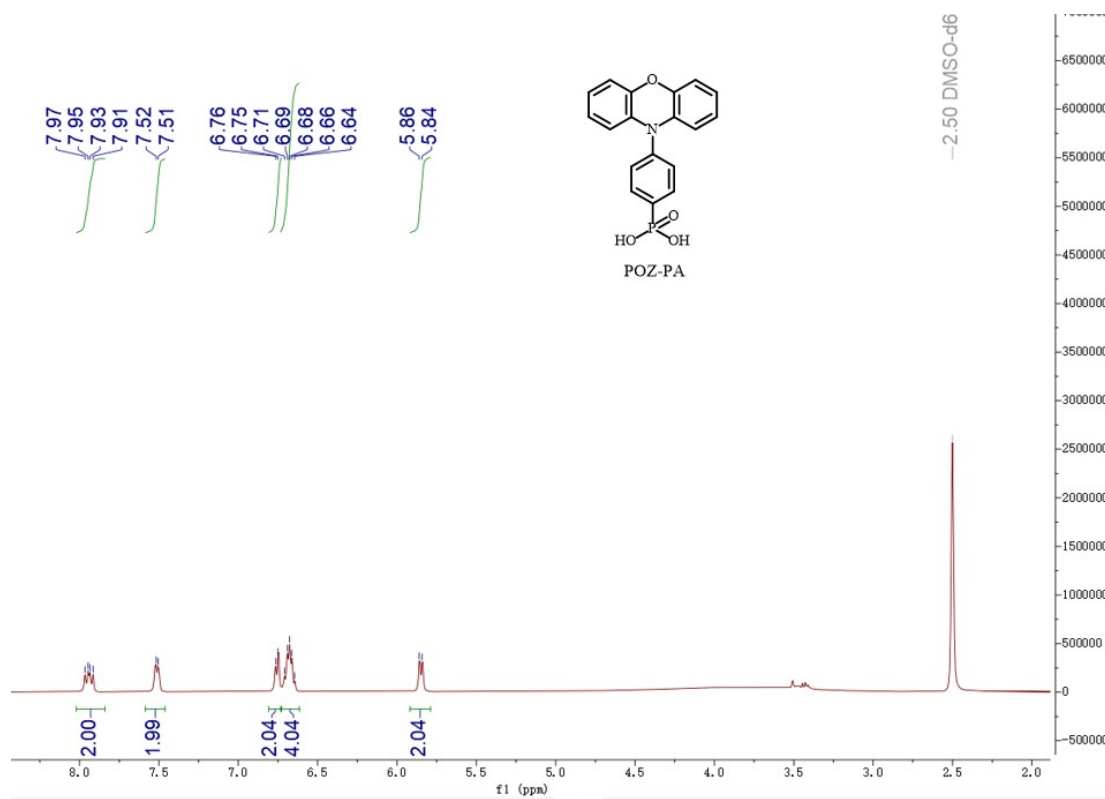
Figure S1. ^{1}H-NMR spectrum of POZ-PA in DMSO-d_6.
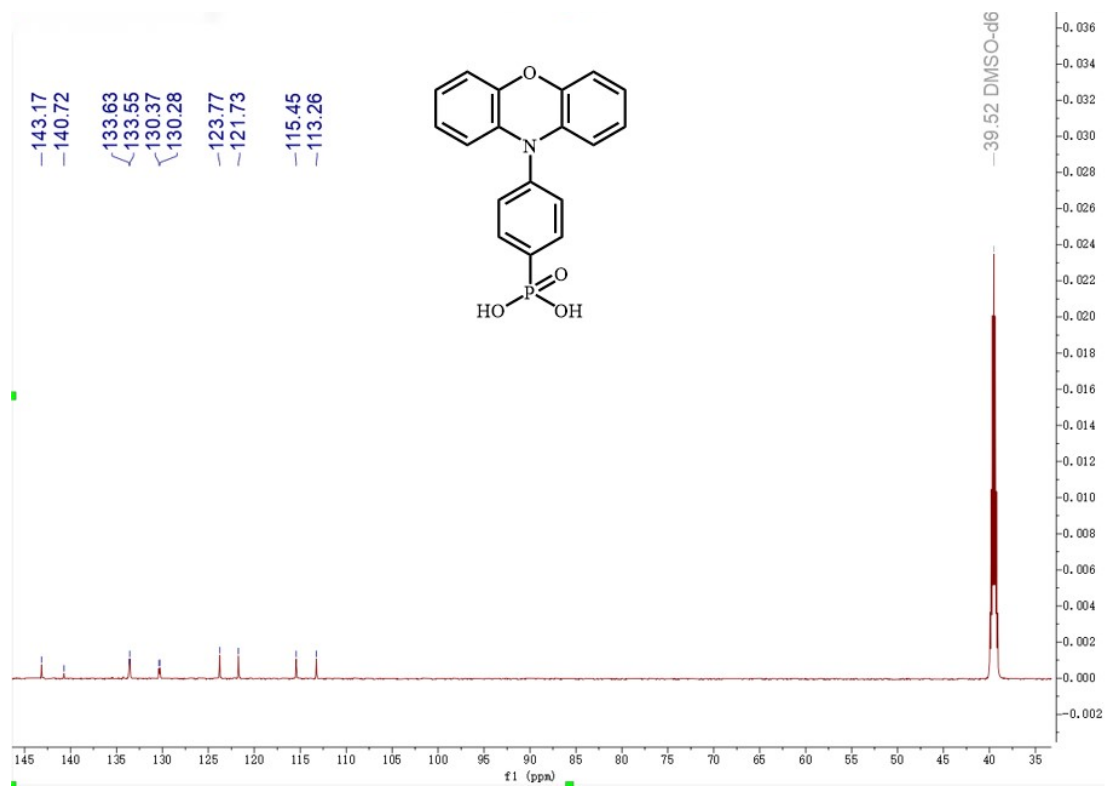
Figure S2. ^{13}C-NMR spectrum of POZ-PA in DMSO-d_6.
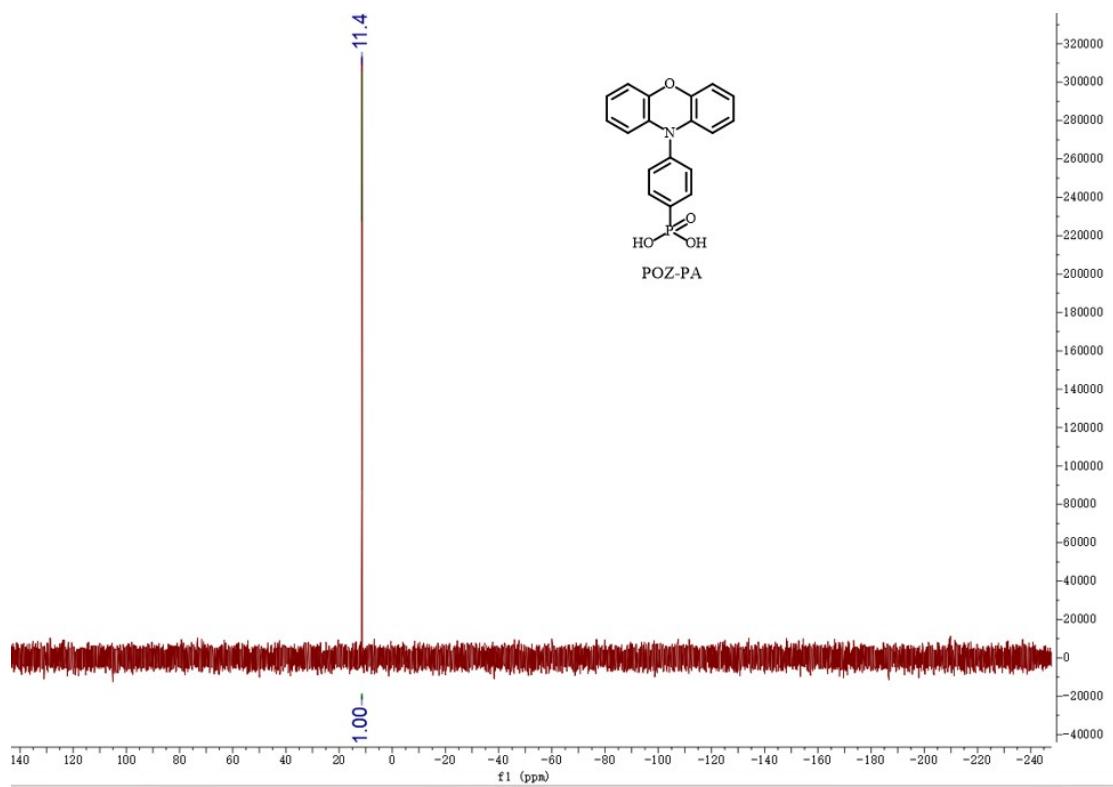
Figure S3. ^{31}P-NMR spectrum of POZ-PA in DMSO-d_6.
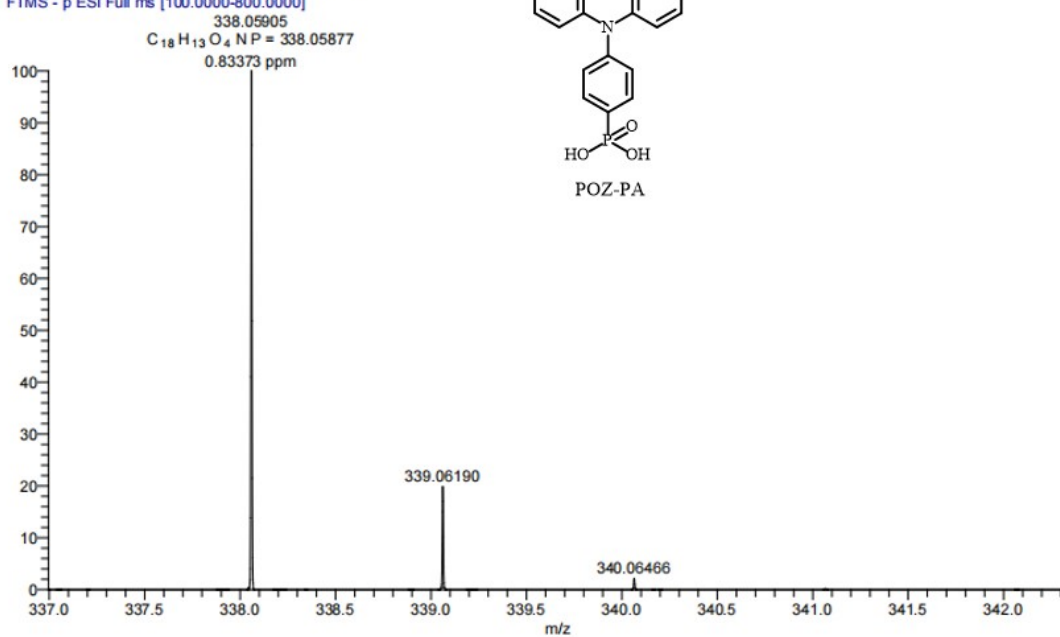
Figure S4. HRMS spectrum of POZ-PA.
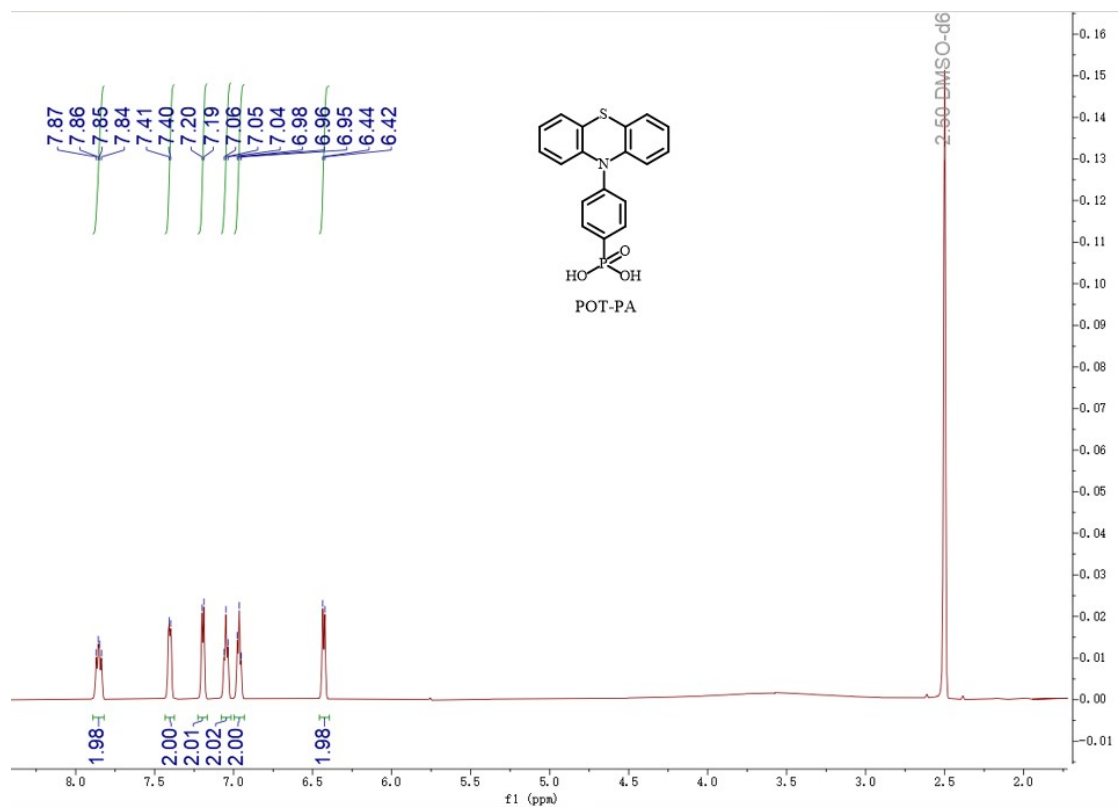
Figure S5. ^{1}H-NMR spectrum of POT-PA in DMSO-d_6.
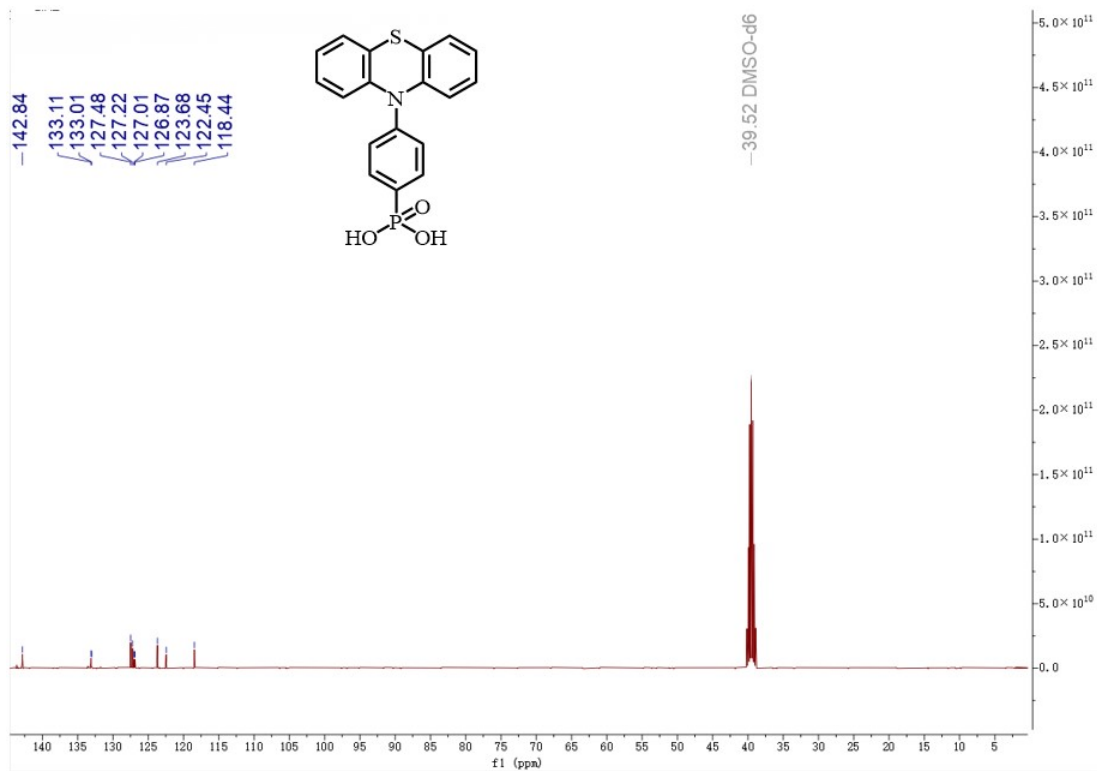
Figure S6. ^{13}C-NMR spectrum of POT-PA in DMSO-d_6.
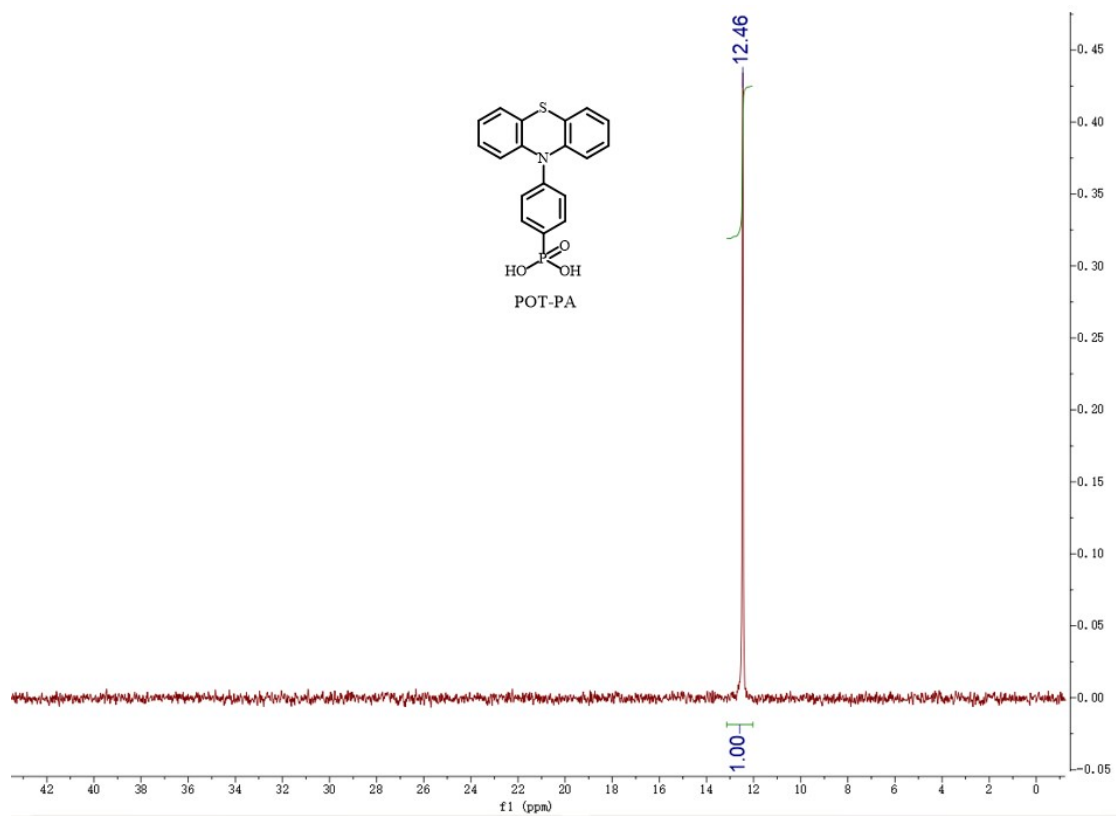
Figure S7. ^{31}P-NMR spectrum of POT-PA in DMSO-d_6.
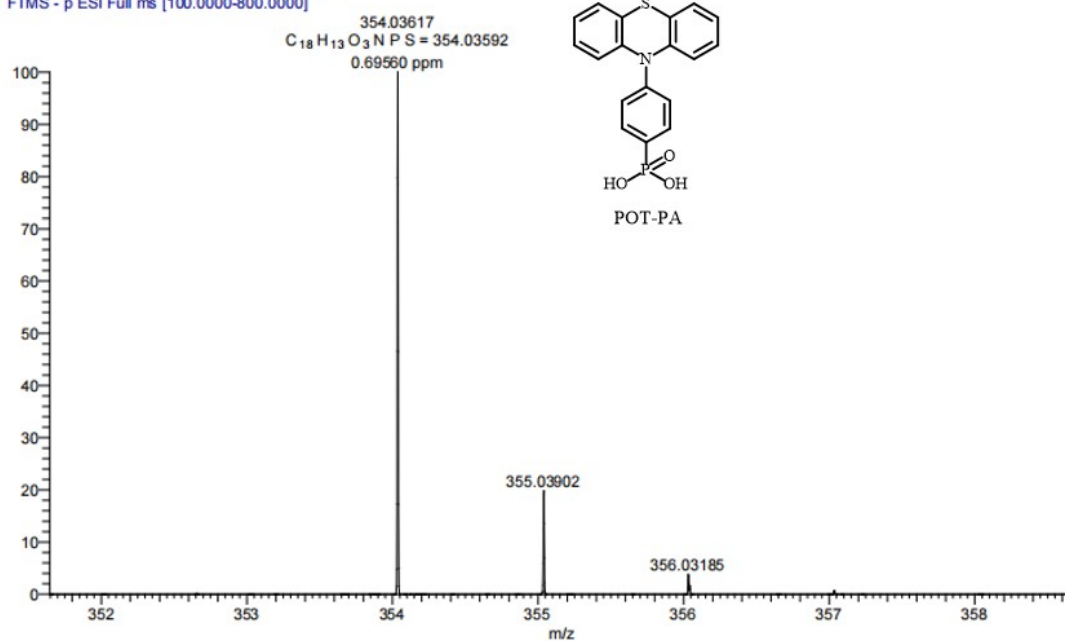
Figure S8. HRMS spectrum of POT-PA.
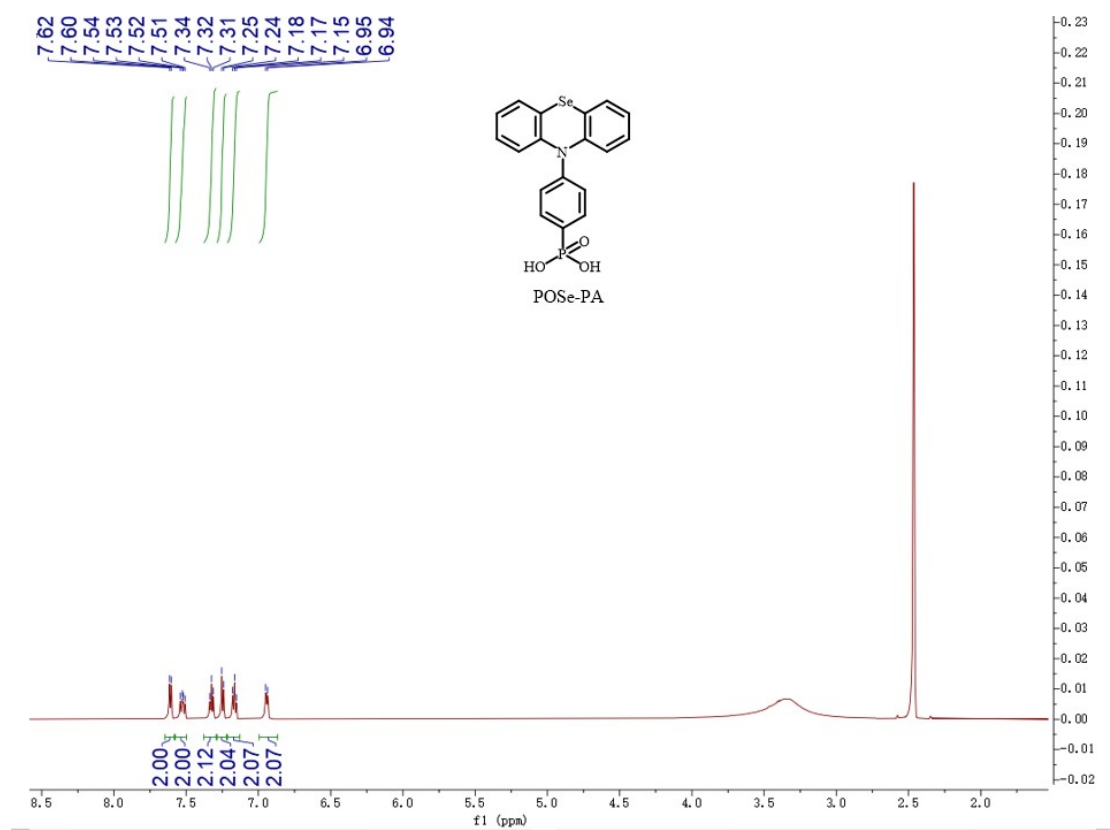
Figure S9. ^{1}H-NMR spectrum of POSe-PA in DMSO-d_6.
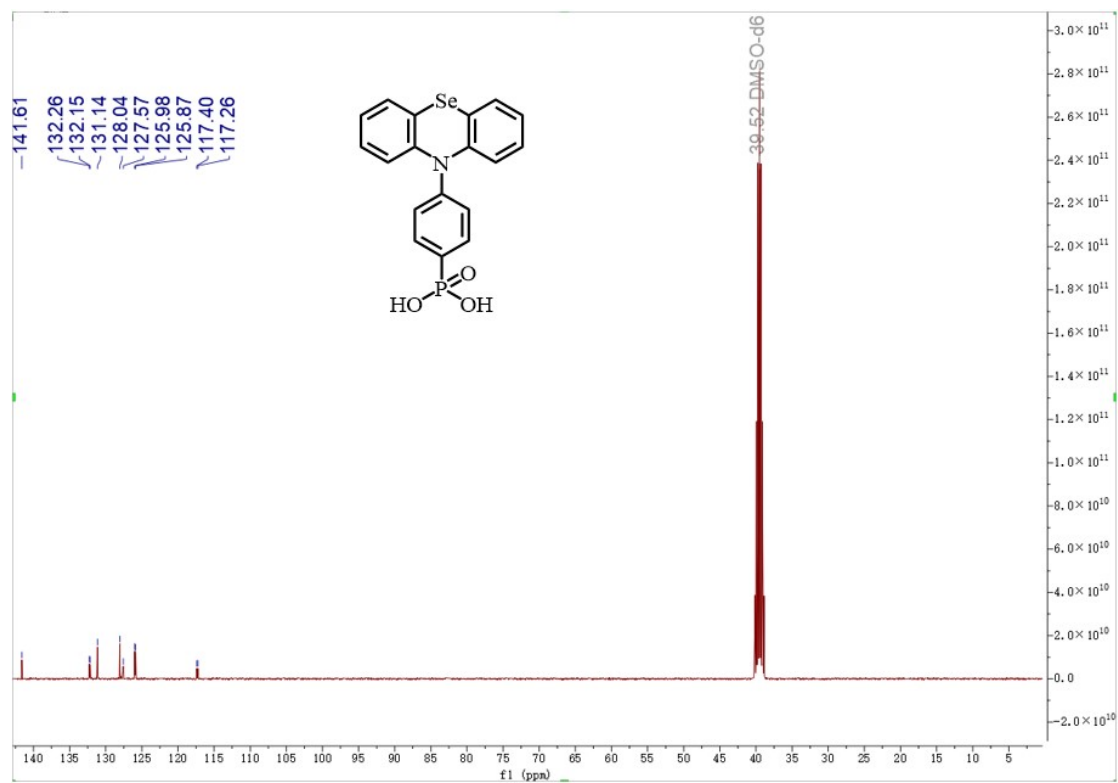
Figure S10. ^{13}C-NMR spectrum of POSe-PA in DMSO-d_6.
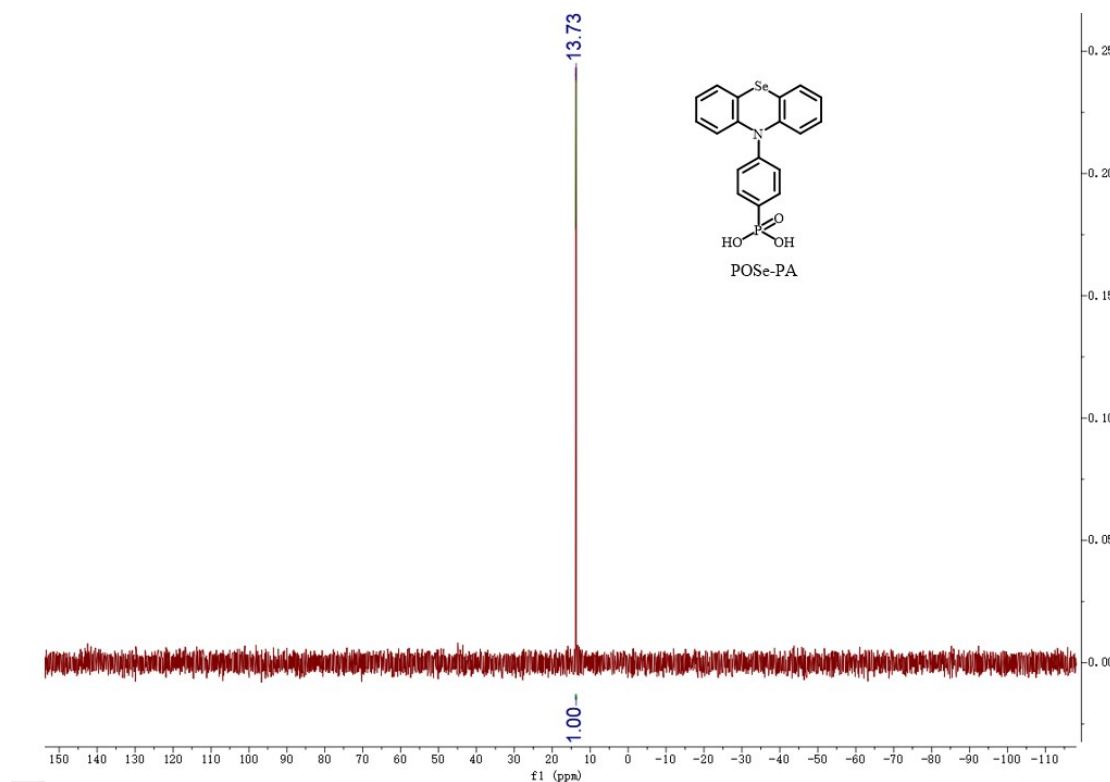
Figure S11. ^{31}P-NMR spectrum of POSe-PA in DMSO-d_6.
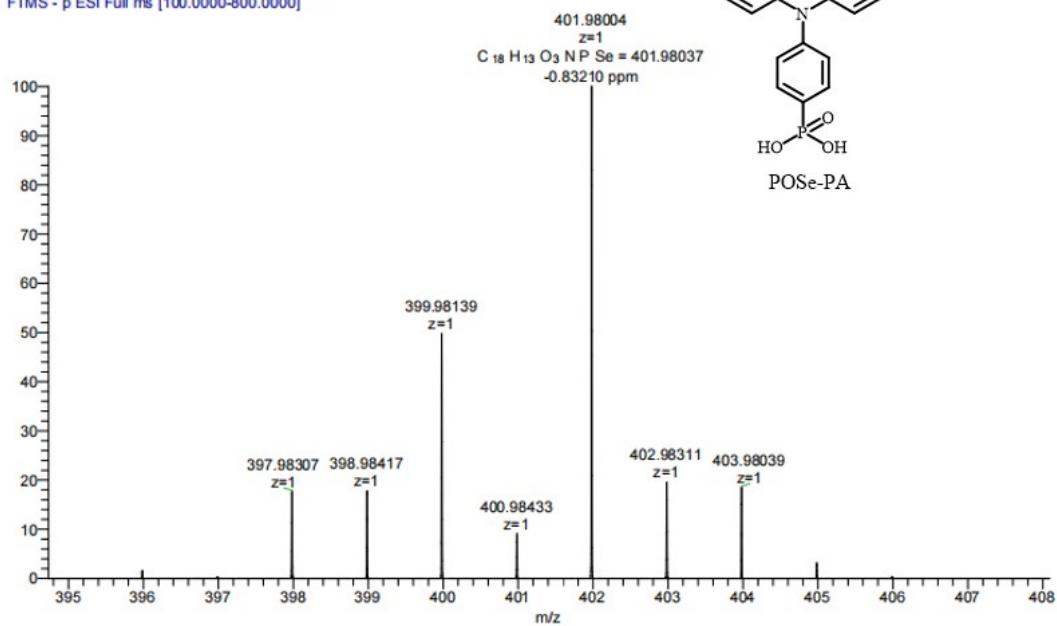
Figure S12. HRMS spectrum of POSe-PA.
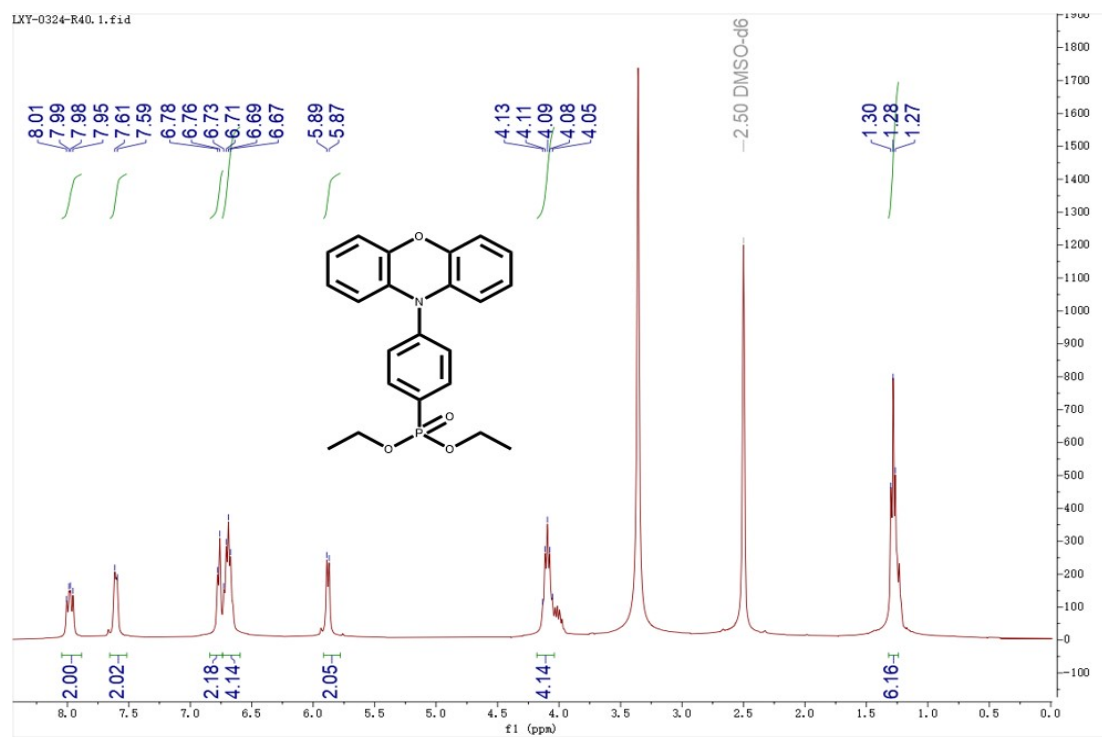
Figure S13. ^{1}H-NMR spectrum of **Compound 2** in DMSO-d_6.

Figure S14. ^{13}C-NMR spectrum of **Compound 2** in CDCl$_3$.
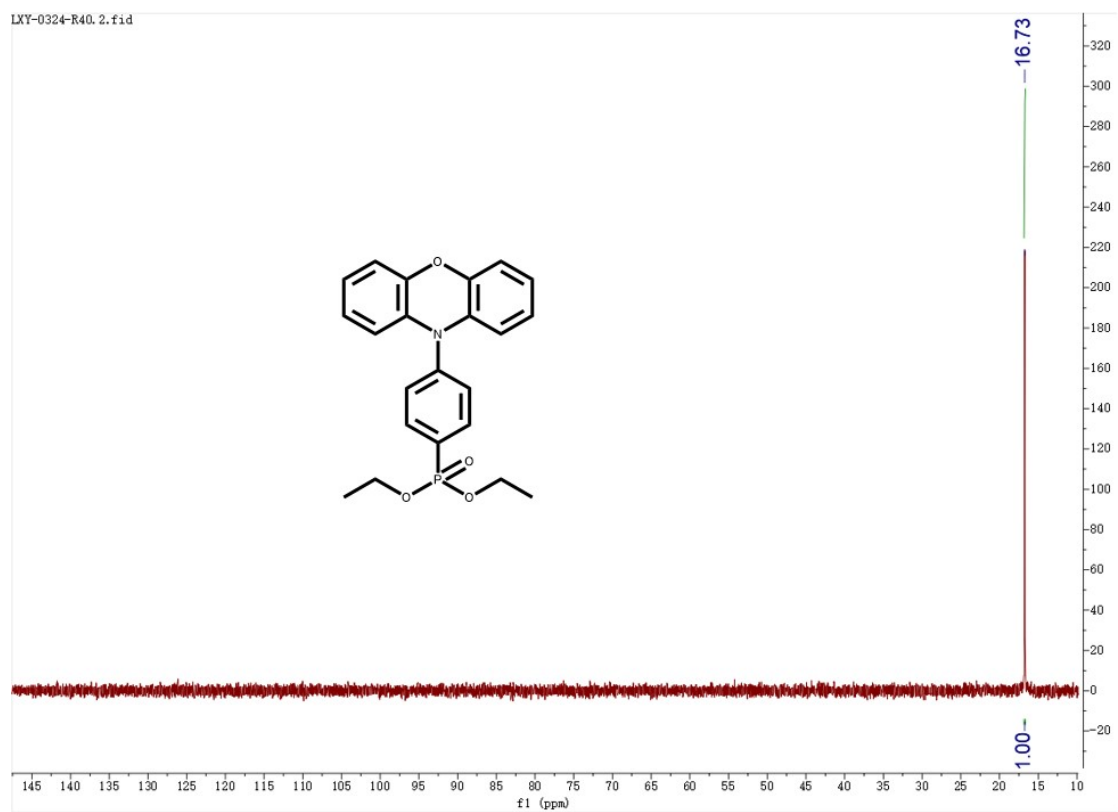
Figure S15. ^{31}P-NMR spectrum of **Compound 2** in DMSO-d_6.

Zoom in, [M+H]⁺
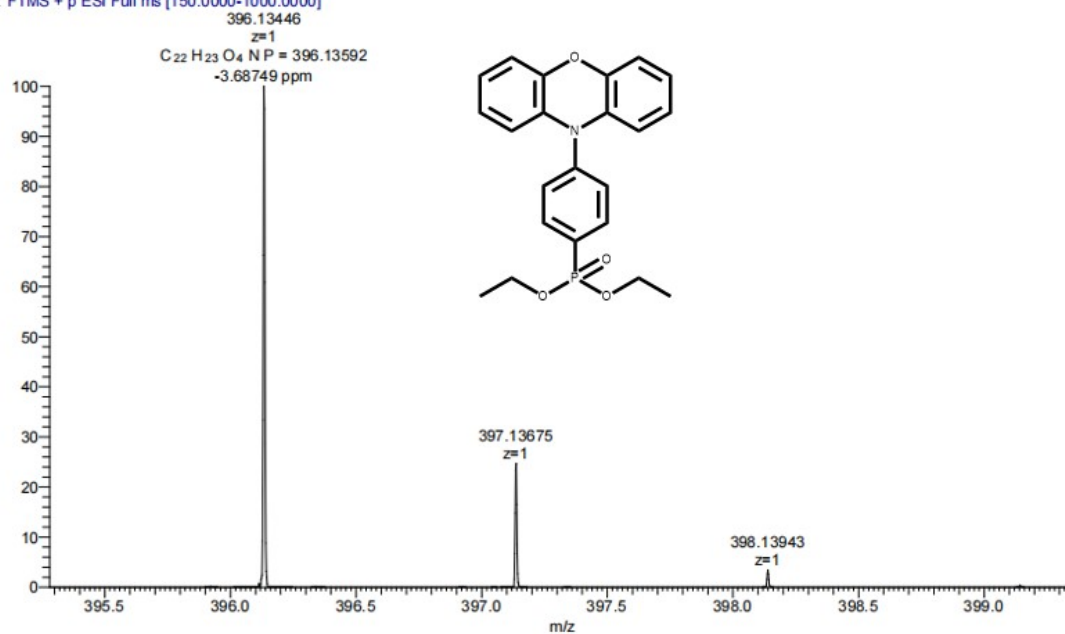
Figure S16. HRMS spectrum of **Compound 2**.
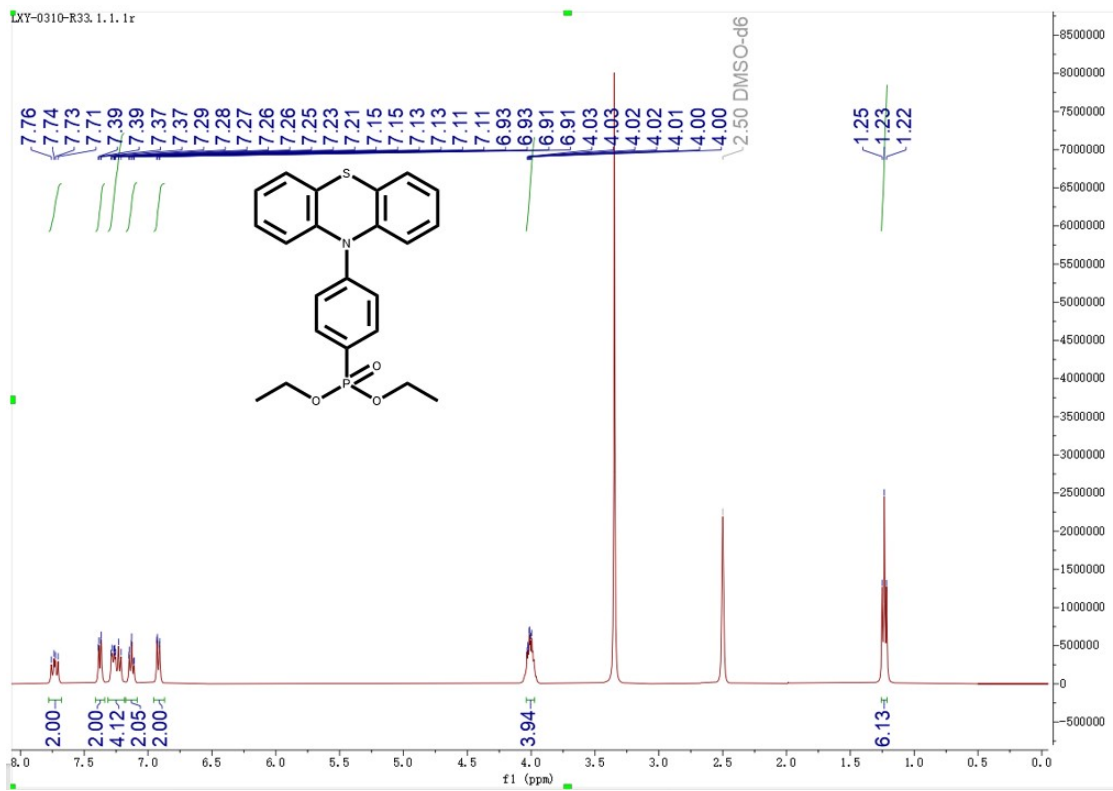
Figure S17. ^{1}H-NMR spectrum of **Compound 4** in DMSO-d_6.
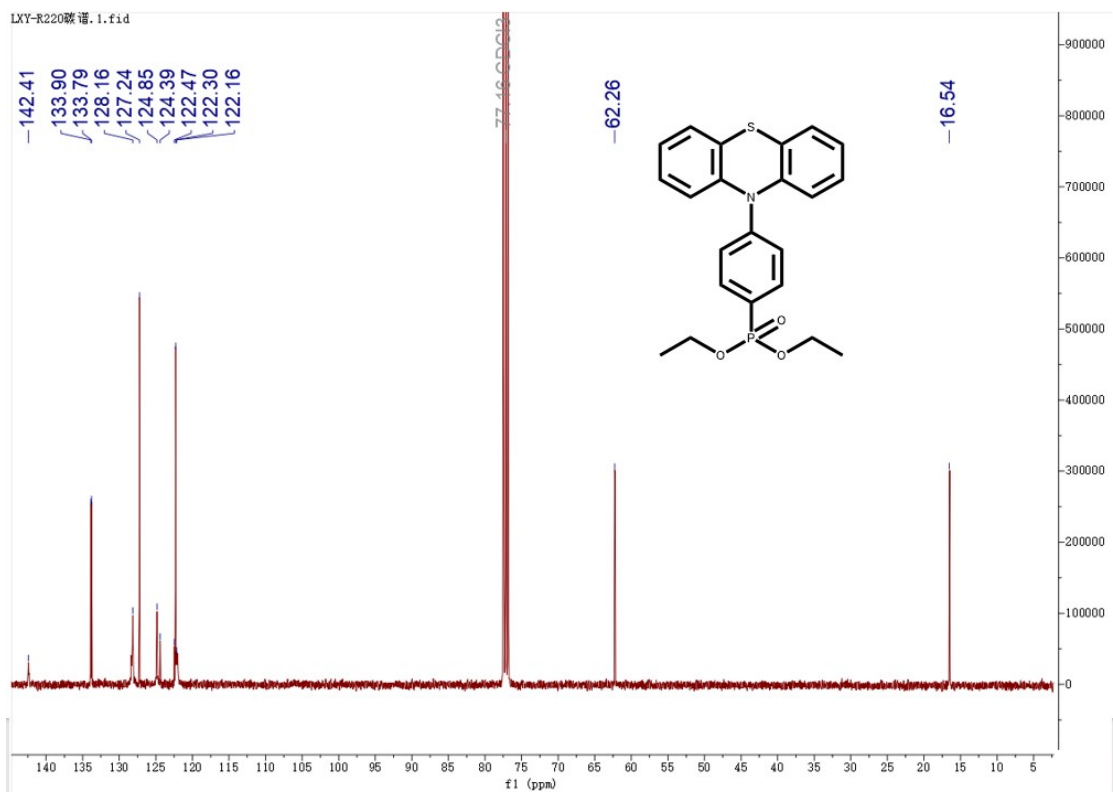
Figure S18. ^{13}C-NMR spectrum of **Compound 4** in CDCl$_3$.
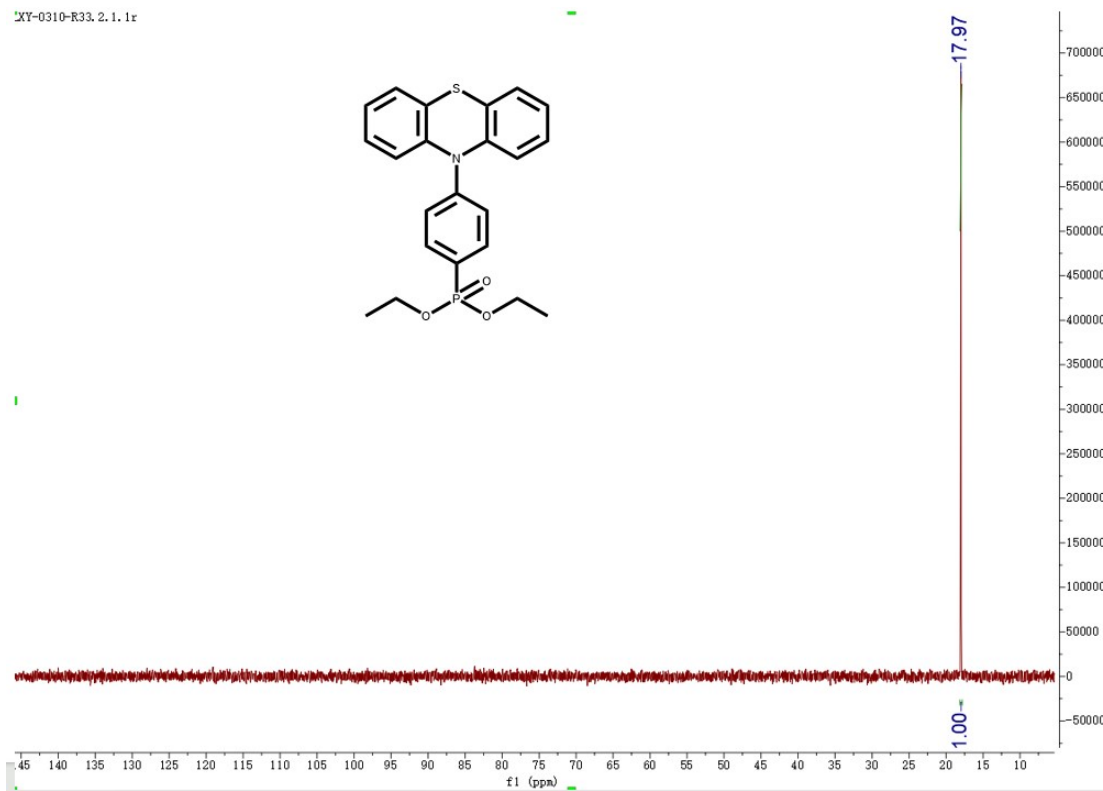
Figure S19. ^{31}P-NMR spectrum of **Compound 4** in DMSO-d_6.

Zoom in, [M+H]⁺
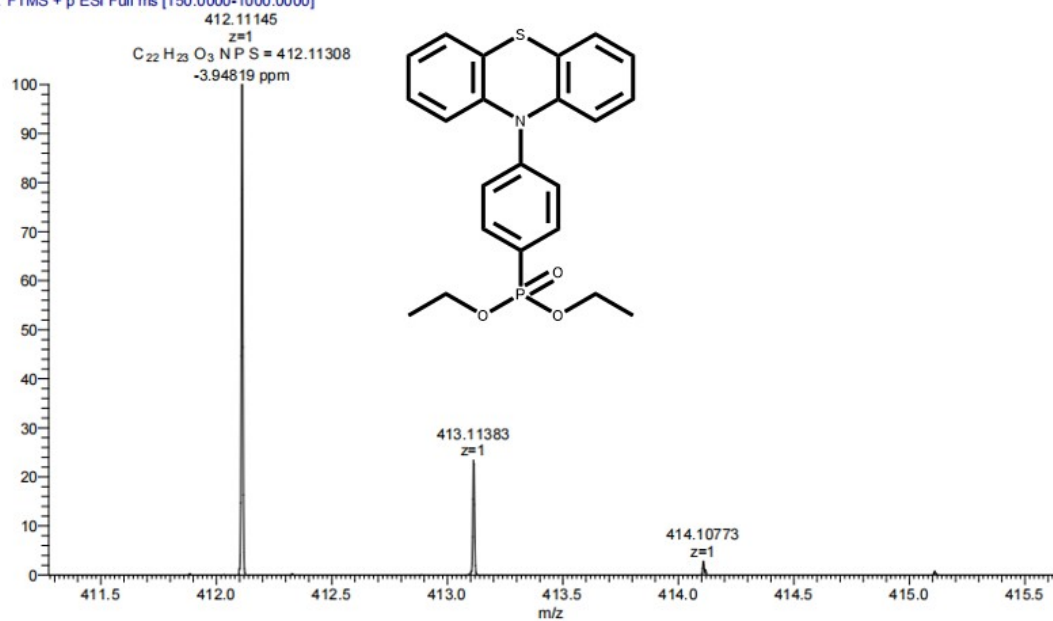
Figure S20. HRMS spectrum of **Compound 4**.
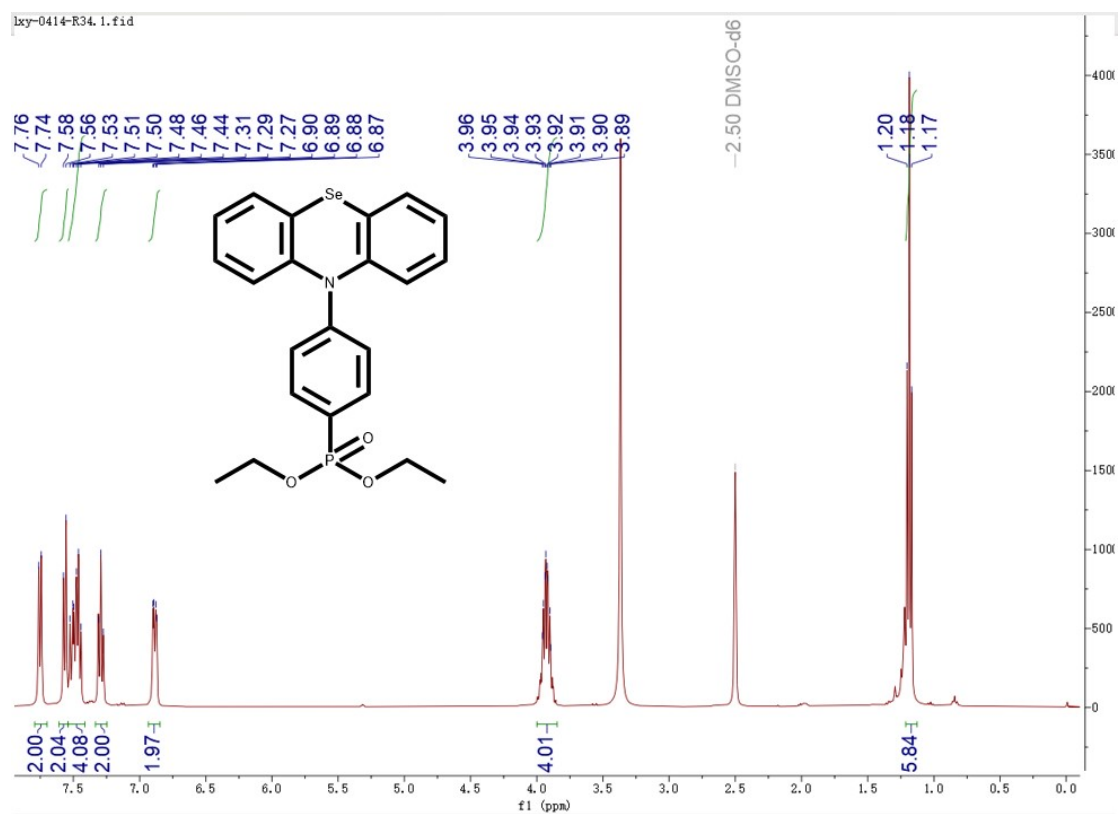
Figure S21. ^{1}H-NMR spectrum of **Compound 9** in DMSO-d_6.
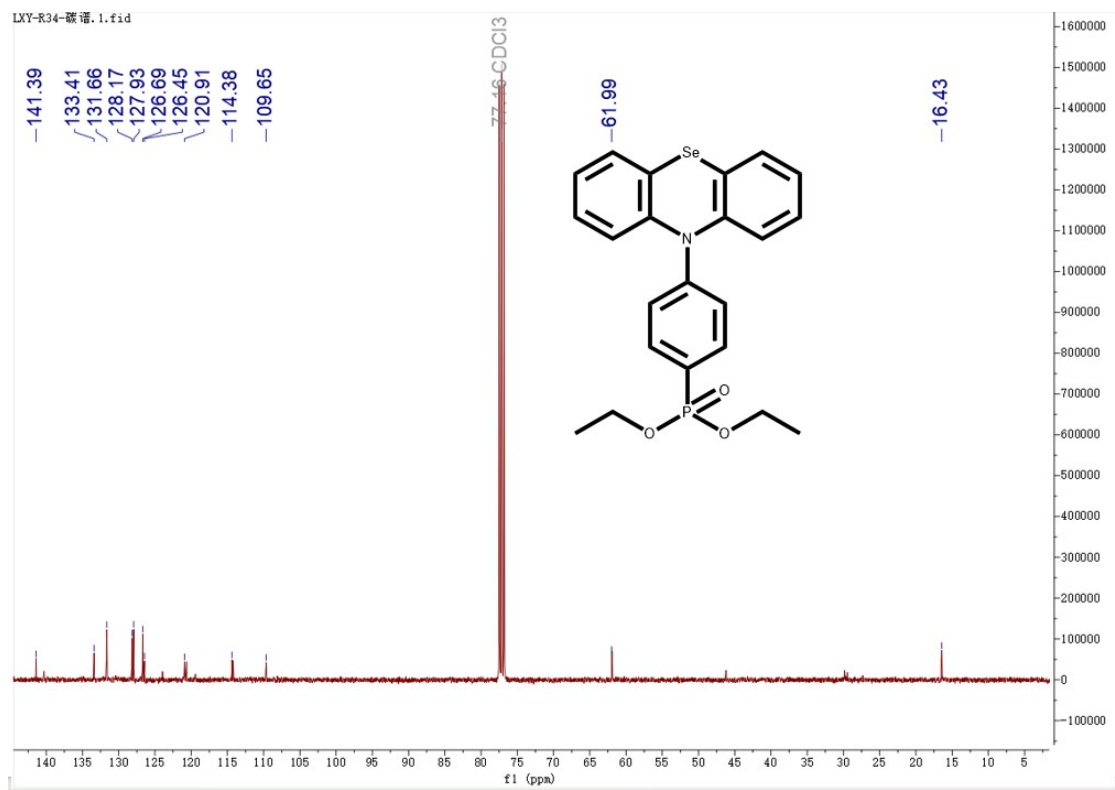
Figure S22. ^{13}C-NMR spectrum of **Compound 9** in CDCl$_3$.
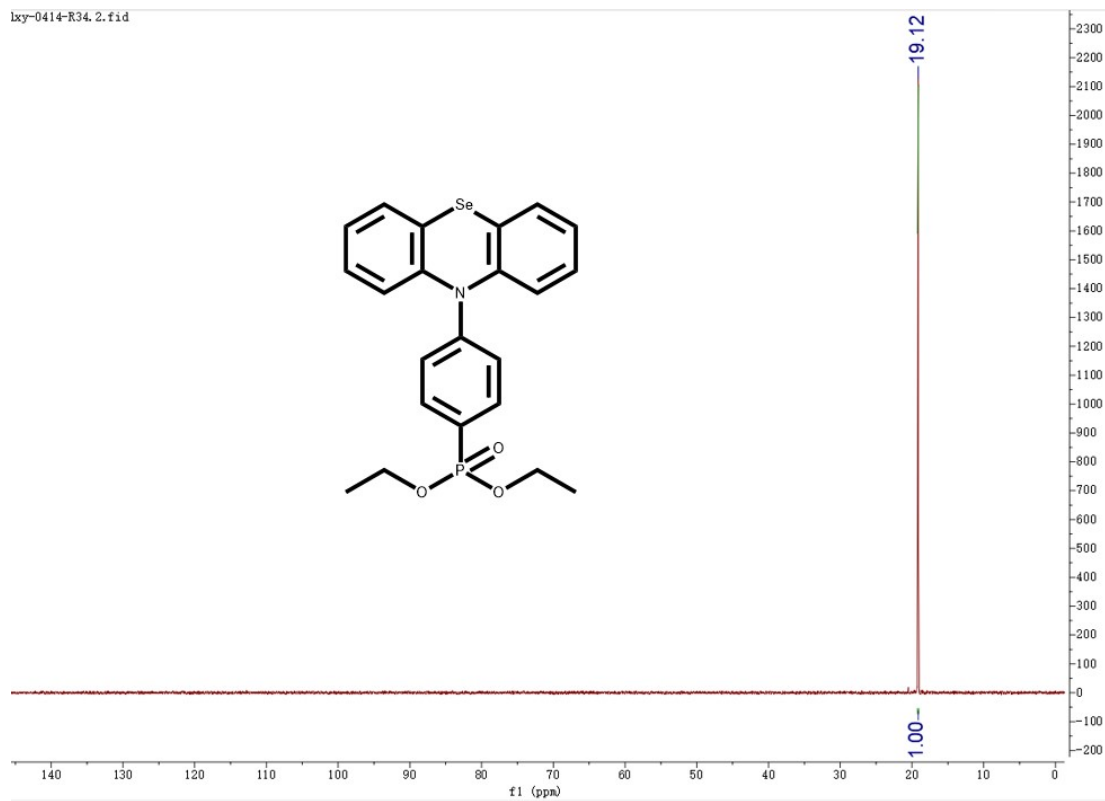
Figure S23. ^{31}P-NMR spectrum of **Compound 9** in DMSO-d_6.
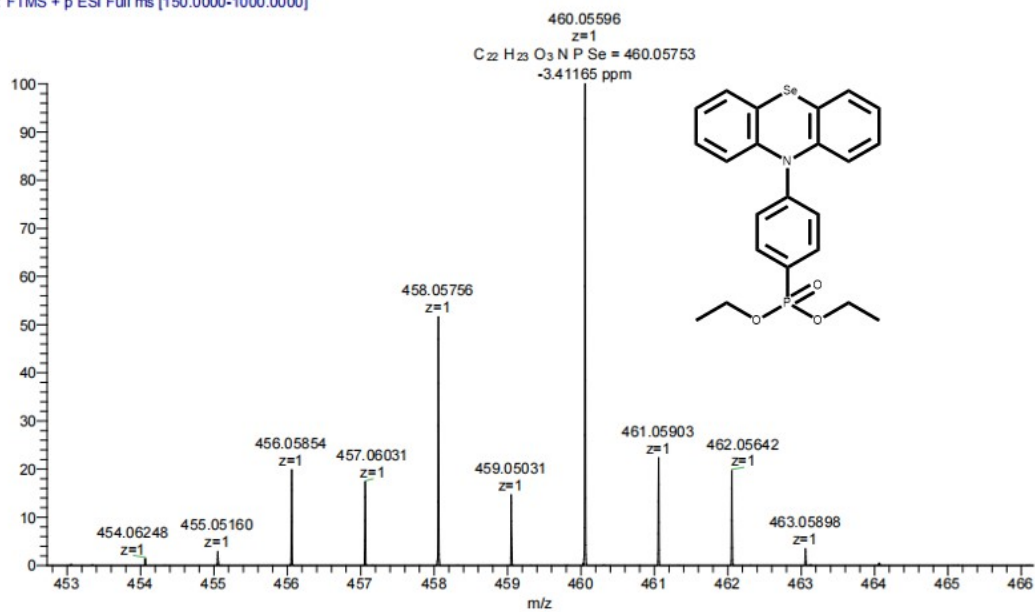
Figure S24. HRMS spectrum of **Compound 9**.
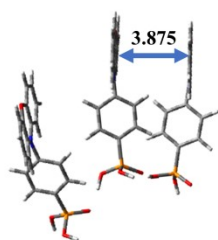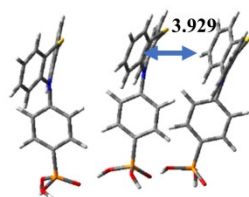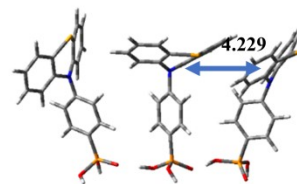
POZ-PA   **POT-PA**   **POSe-PA**

Figure S25. Optimized stacking models of SAMs on DFT calculations.

	POZ-PA	POT-PA	POSe-PA
HOMO	-5.03 eV	-5.30eV	-5.33eV
LUMO	-1.56eV	-1.54eV	-1.52eV
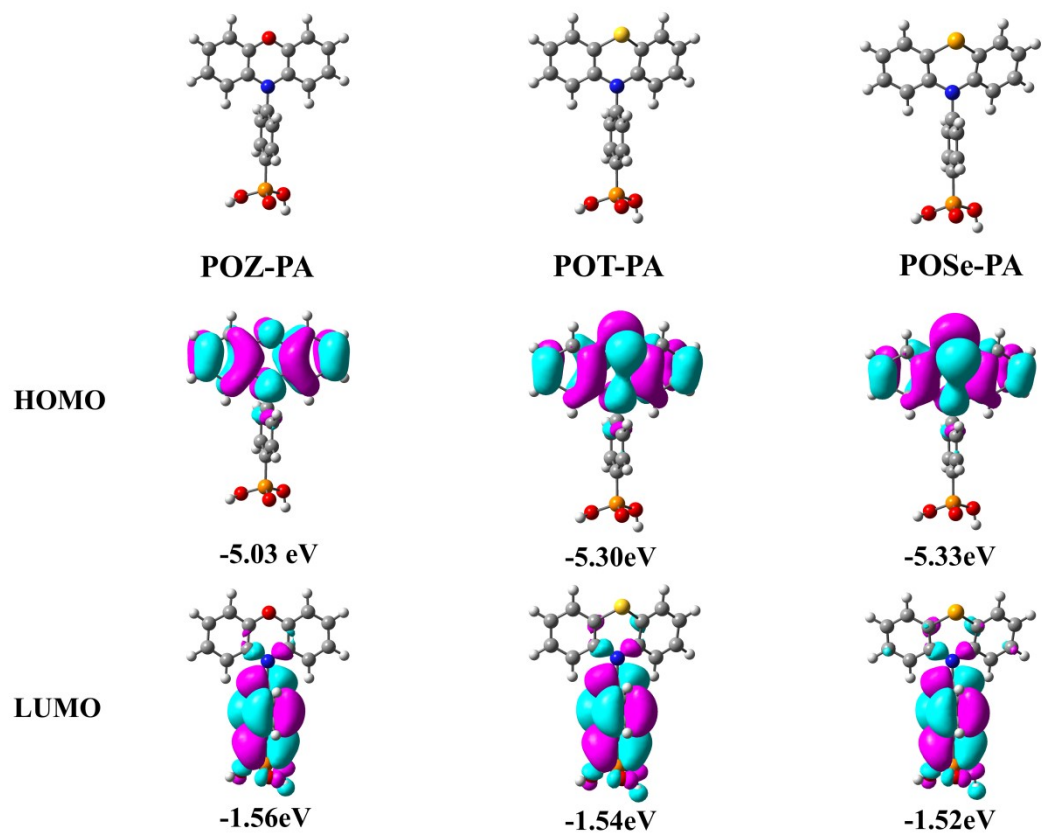
Figure S26. Commutated frontier molecular orbital distributions of POZ-PA, POT-PA, and POSe-PA by B3LYP/6-31G (d, p).
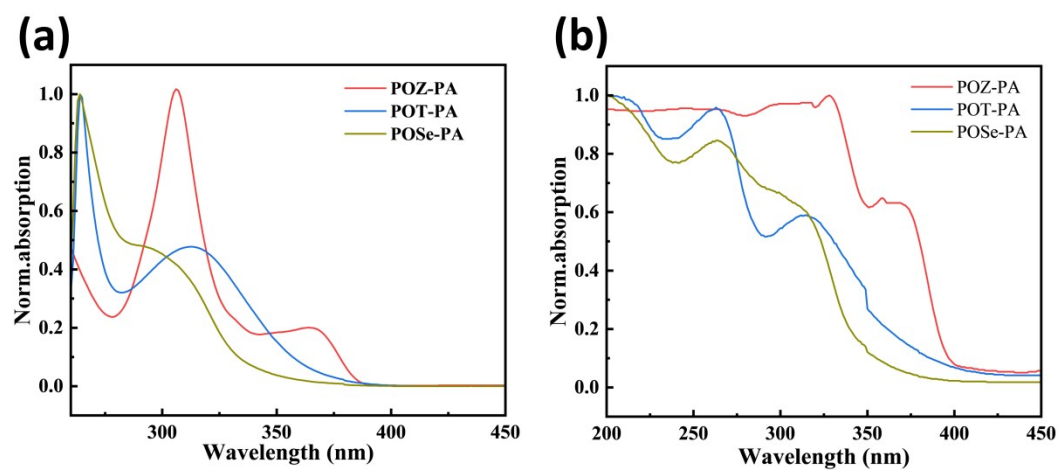
Figure S27. Ultraviolet-visible (UV-vis) (a) absorption coefficients of POZ-PA, POT-PA, and POSe-PA solutions (solvent: DMF, concentration: 10^{-5} mol·L^{-1}) and (b) thin films (concentration: 2 mg·mL^{-1}).
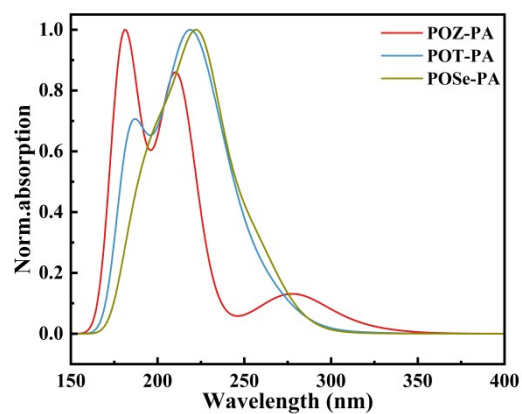
Figure S28. The simulated UV-vis absorption spectra of POZ-PA, POT-PA, and POSe-PA using DFT calculations.
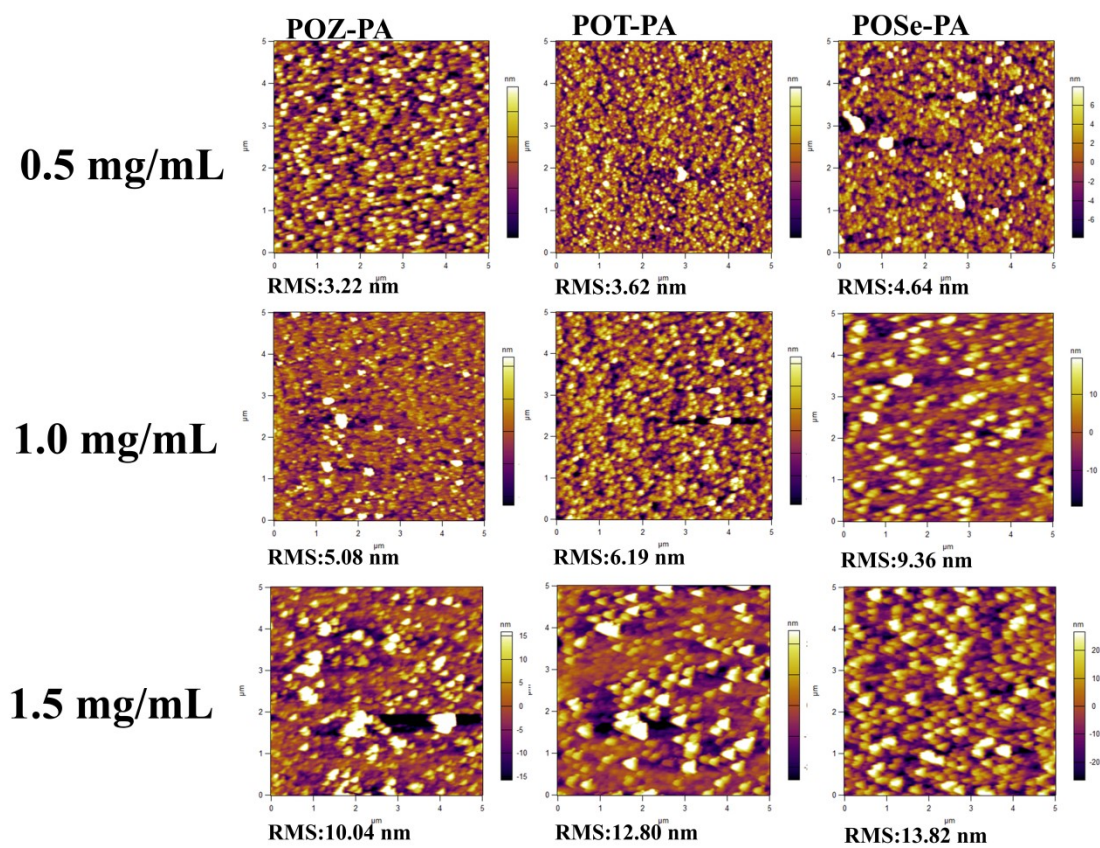
Figure S29. AFM characterization of thin films fabricated from three SAMs with solution concentrations of 0.5, 1, and 1.5 mg/mL.
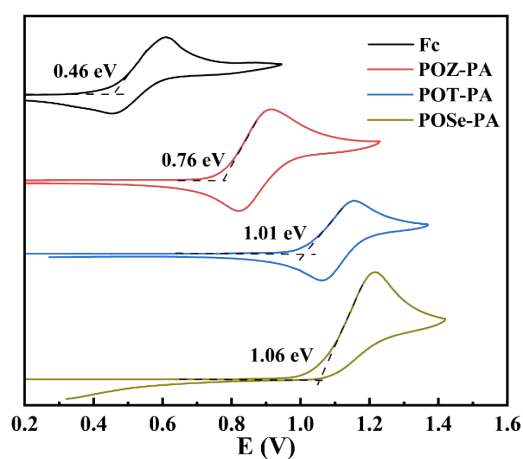
Figure S30. Cyclic voltammetry characterized oxidation potential of phosphates corresponding to POZ-PA, POT-PA and POSe-PA in (1×10^{-3} mol·L^{-1}) in DMF with 0.1M Bu$_4$NPF$_6$ as electrolyte, glassy carbon and platinum wire as working and counter electrodes and Ag/AgCl as reference electrode; scanning rate was 100 mv·s^{-1}; Ferrocene was used as external reference and the potentials were presented by reference to E$_{1/2}$(Fc/Fc$^+$).
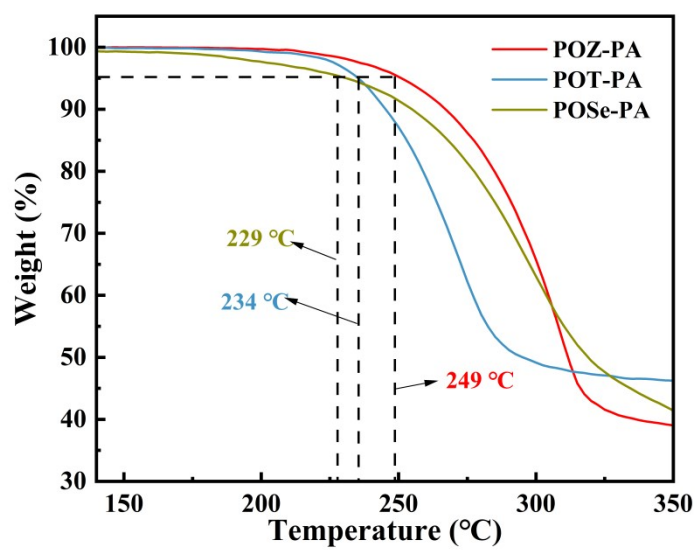
Figure S31. TGA curves of POZ-PA, POT-PA, and POSe-PA.
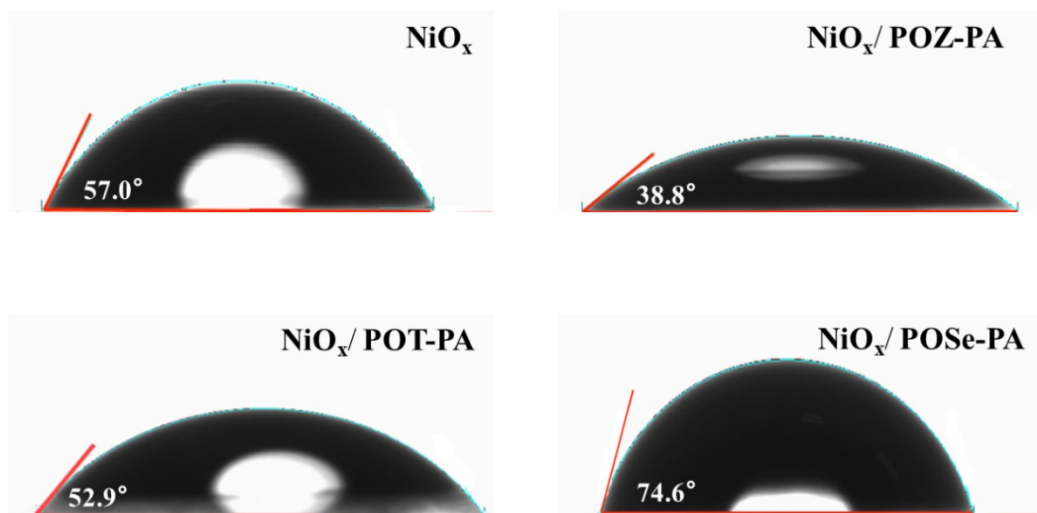
Figure S32. Water contact angles (WCAs) of NiO_x/SAMs samples.

NiO$_x$

NiO$_x$/POZ-PA

24.7°

14.9°

NiO$_x$/POT-PA

NiO$_x$/POSe-PA

16.7°

19.7°
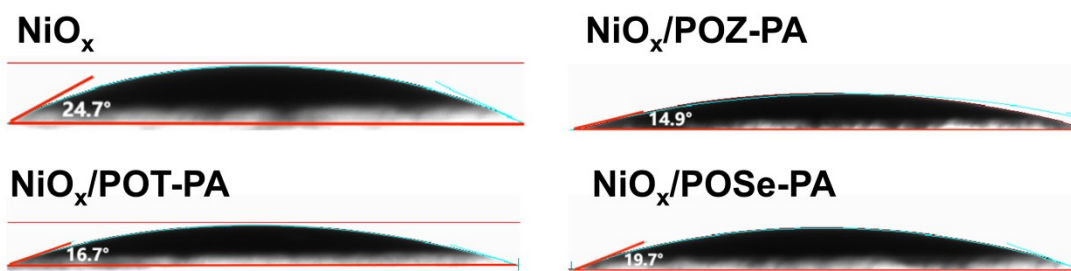
Figure S33. Contact angle of perovskite precursor solution of NiO$_x$/SAMs samples.
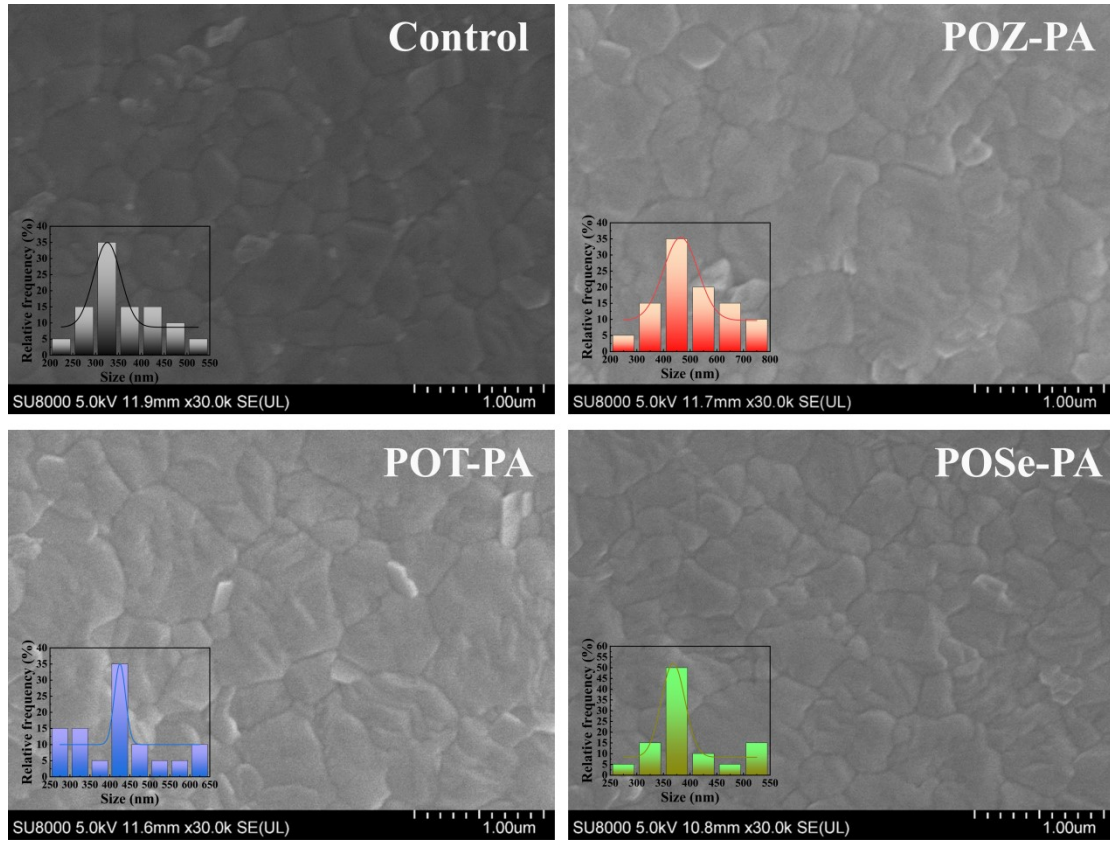
Figure S34. Surface topographic SEM images of the perovskite films deposited on control group, POZ-PA, POT-PA, and POSe-PA.
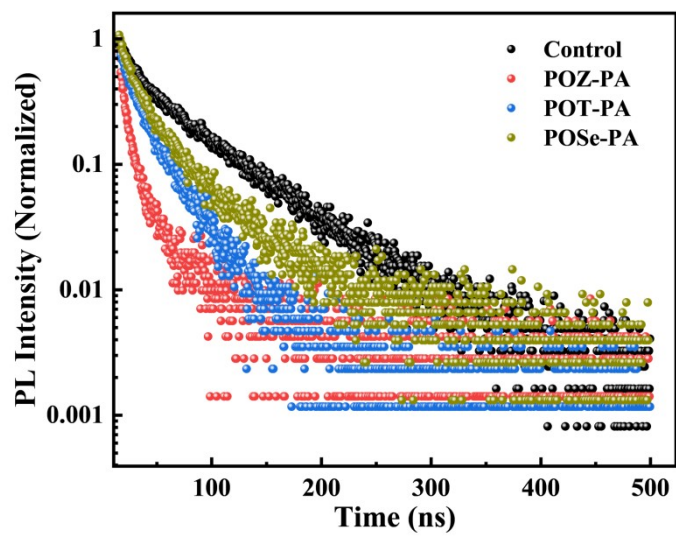
Figure S35. TRPL spectra of NiO_x/perovskite and NiO_x/SAMs/perovskite films.
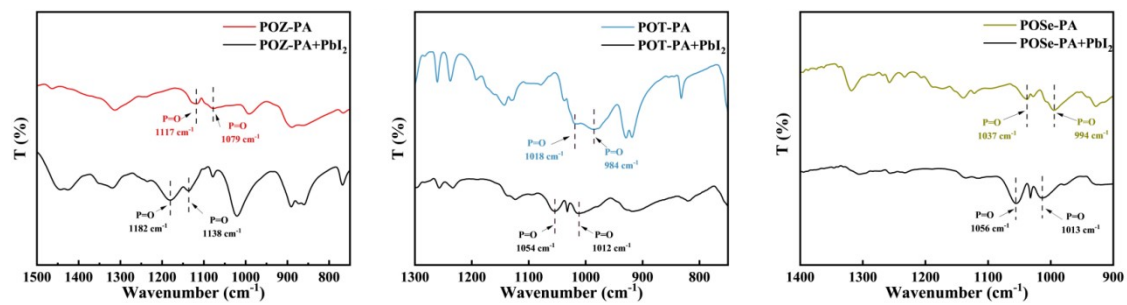
Figure S36. FTIR spectra of POZ-PA, POT-PA, and POSe-PA with or without PbI$_2$.
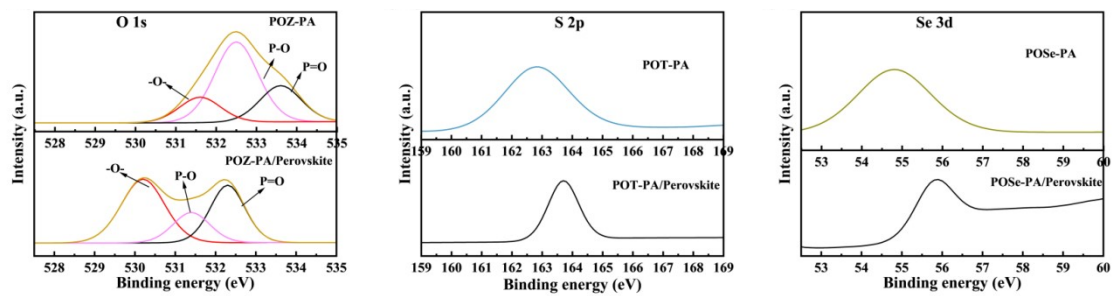
Figure S37. The XPS results of O 1*s* of POZ-PA, S 1*p* of POT-PA, and Se 3*d* of POSe-PA with or without Perovskite.
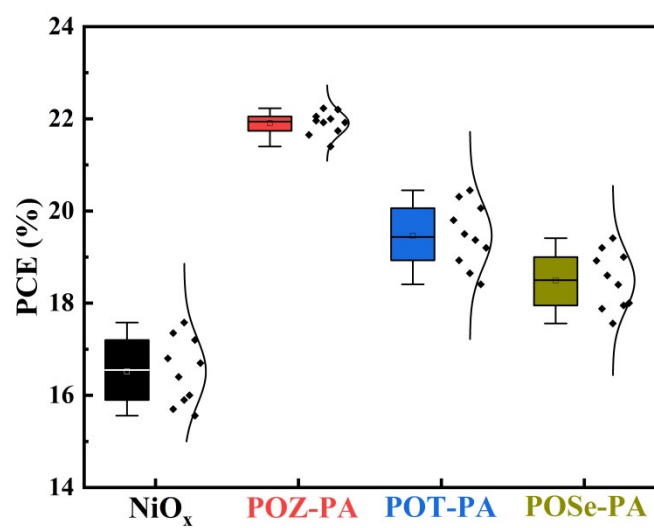
Figure S38. Box plot distribution of PCE values for ten identical sample groups.
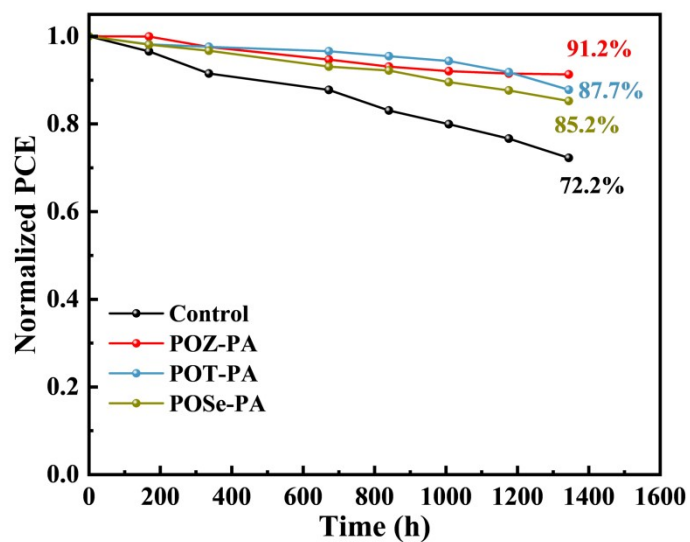
Figure S39. Storage stability of PSCs with different hole-selective layers stressed continuously at room temperature in an inert environment without encapsulation.

Table S1. TRPL lifetime for perovskite films with different HSCs.

TRPL lifetime	A_1	τ_1 (ns)	A_2	τ_2 (ns)	τ_{avg} (ns)
NiO$_x$	0.67	14.41	0.33	63.15	47.41
NiO$_x$/POZ-PA	0.80	6.03	0.20	32.31	21.08
NiO$_x$/POT-PA	0.73	10.20	0.27	36.32	25.13
NiO$_x$/POSe-PA	0.74	9.57	0.26	41.12	28.54

The TRPL decays were fitted with a biexponential decay function $y = y_0 + A_1 \times e^{(-x/\tau_1)} + A_2 \times e^{(-x/\tau_2)}$, and the τ_{avg} is calculated through equation of $\tau_{avg} = (A_1\tau_1^2 + A_2\tau_2^2)/(A_1\tau_1 + A_2\tau_2)$

References:

[1] In Seob Park , Sae Youn Lee , Chihaya Adachi , Takuma Yasuda, *Adv. Funct. Mater*. **2016**, 26, 1813–1821.

[2] M.-H. Yu, X. Liu, Y.-C. Tseng, I. C. Ni, B.-H. Lin, Y. Wang, C.-C. Chueh, *Nano Energy* **2024**, *132,* 110405.

[3] C. Cremer, M. Goswami, C. K. Rank, B. de Bruin, F. W. Patureau, *Angew. Chem. Int. Ed*. **2021**, *60*, 6451.

[4] C. Cremer, M. A. Eltester, H. Bourakhouadar, I. L. Atodiresei, F. W. Patureau, *Org. Lett*. **2021**, *23*, 3243.

[5] J. V. M. J. Frisch, H. P. Hratchian, J. V. Car, Gaussian 09, Revision A.; Gaussian, Inc.: Wallingford, CT, **2009**.

[6] T. Lu, F. Chen, *J. Comput. Chem*. **2012**, *33*, 580.

[7] R. H. Bube, *J. Appl. Physics* **1962**, *33,* 1733.